

Electronic supplementary information

Atomic Insight into Effects of Precursor Clusters on Monolayer WSe₂

Yanxue Zhang, Yuan Chang, Luneng Zhao, Hongsheng Liu*, Junfeng Gao

Key laboratory of Materials Modification by Laser, Ion and Electron Beams (Dalian

University of Technology), Ministry of Education, Dalian, 116024, China

Corresponding author: (liuhongsheng@dlut.edu.cn)

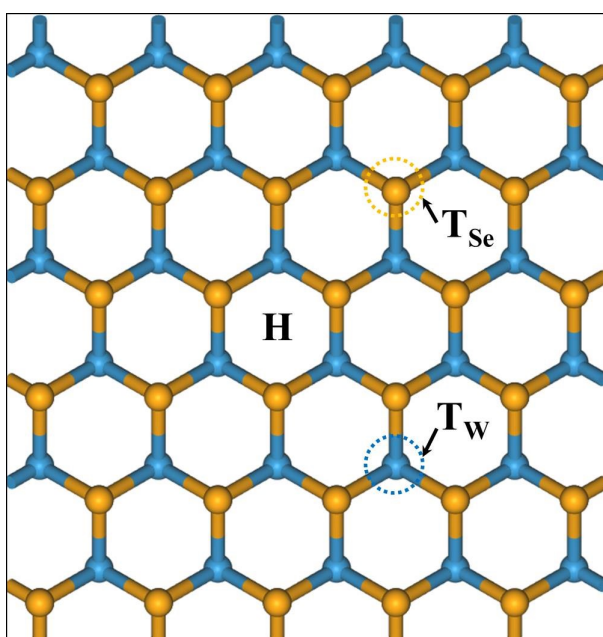


Figure S1. The top view of three different adsorption sites: the top of the Se atom (T_{Se}), the top of the W atom (T_W) and the hollow site (H).

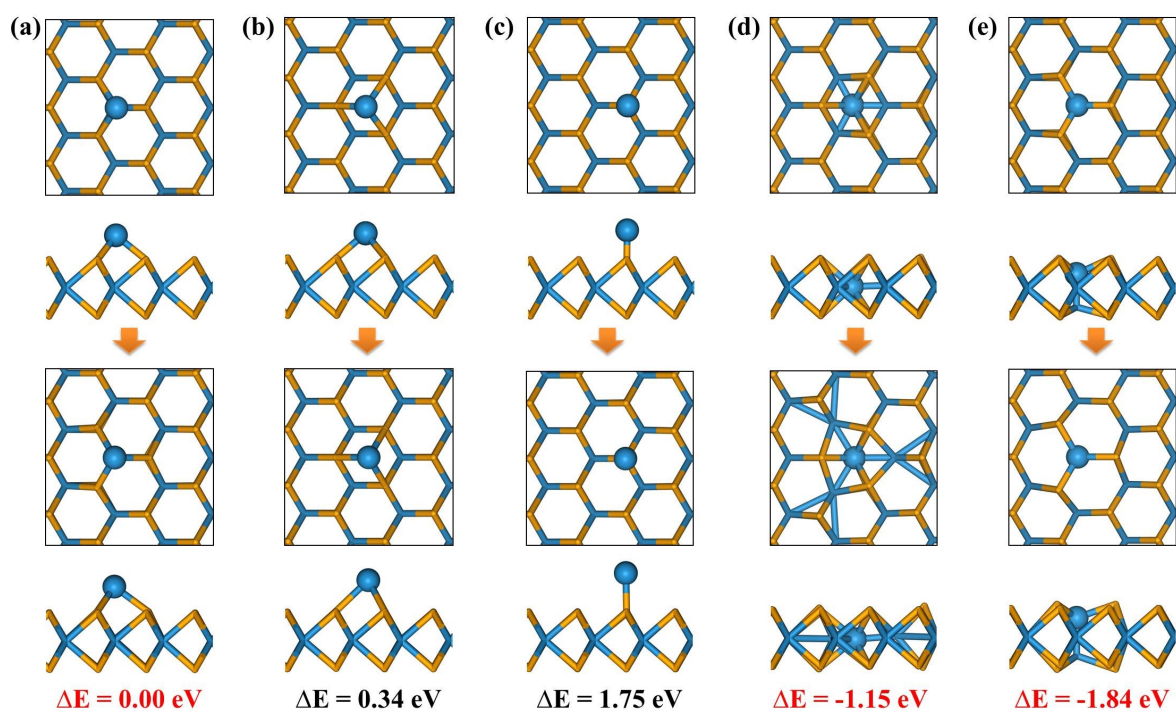


Figure S2. The top and side view of the initial adsorption of single W atoms on the three different adsorption sites (top panel) and the optimized adsorption configuration (bottom panel). The relative energy of the different configurations is also marked. The lowest energy is highlighted in red.

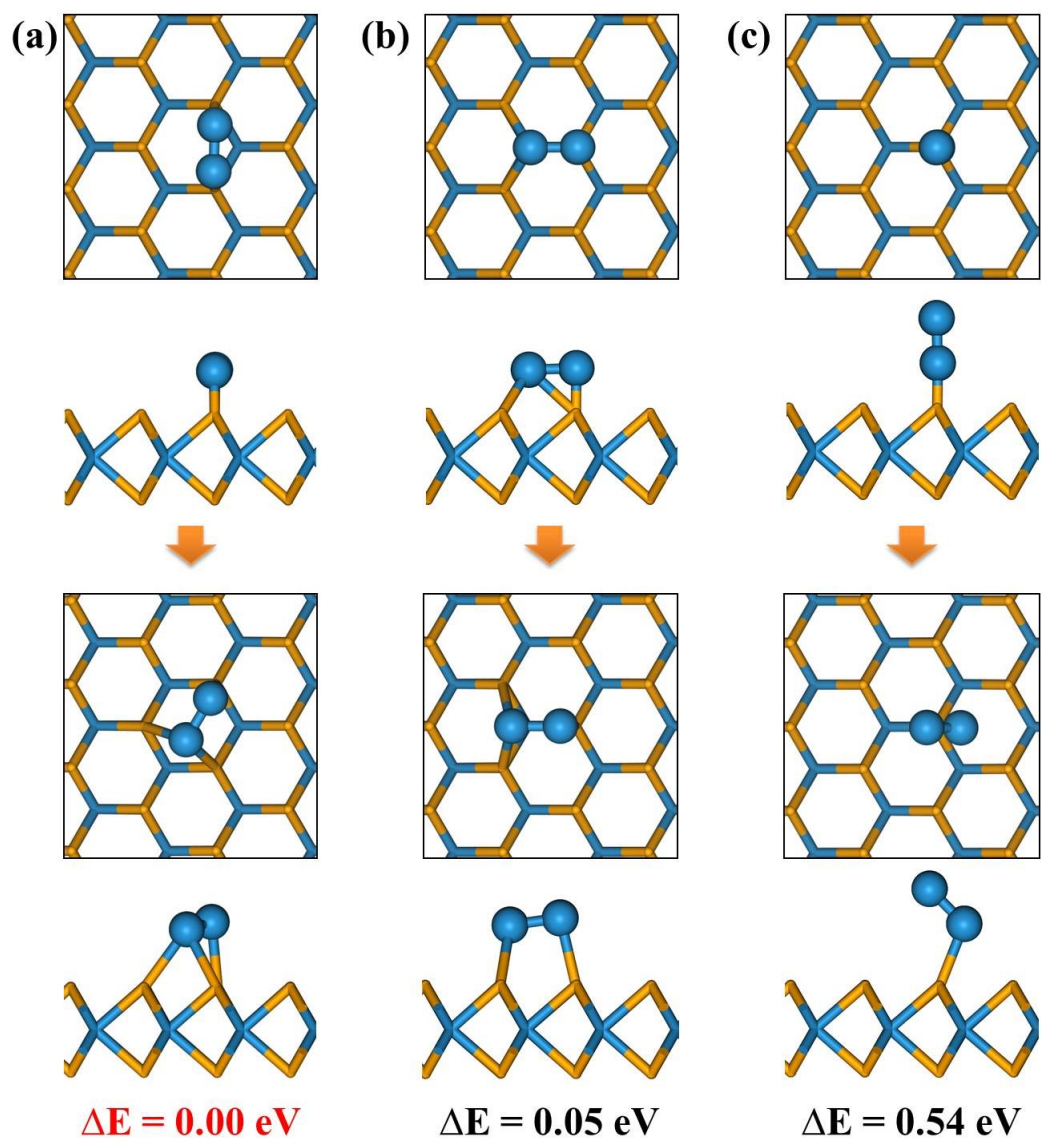


Figure S3. The top and side view of the initial adsorption of W_2 cluster on the three possible adsorption sites (top panel) and the optimized adsorption configuration (bottom panel). The relative energy of the different configurations is also marked. The lowest energy is highlighted in red.

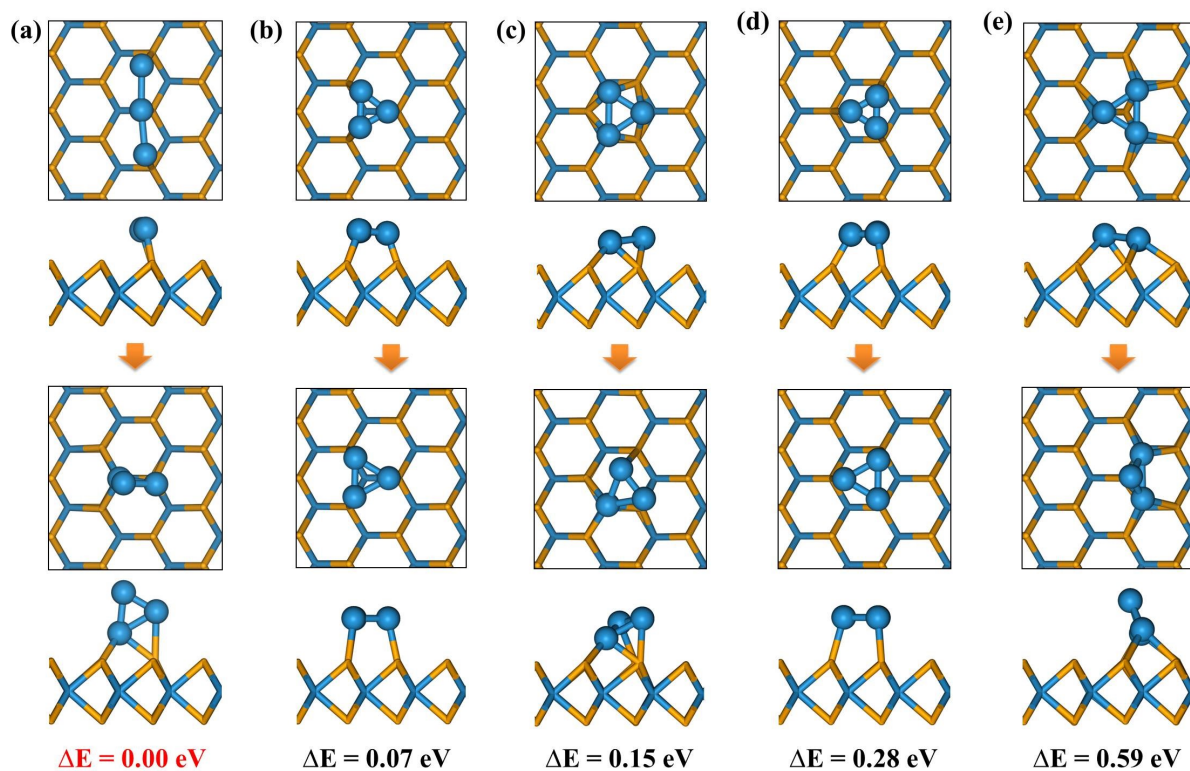


Figure S4. The top and side view of the initial adsorption of W_3 cluster on the five possible adsorption sites (top panel) and the optimized adsorption configuration (bottom panel). The relative energy of the different configurations is also marked. The lowest energy is highlighted in red.

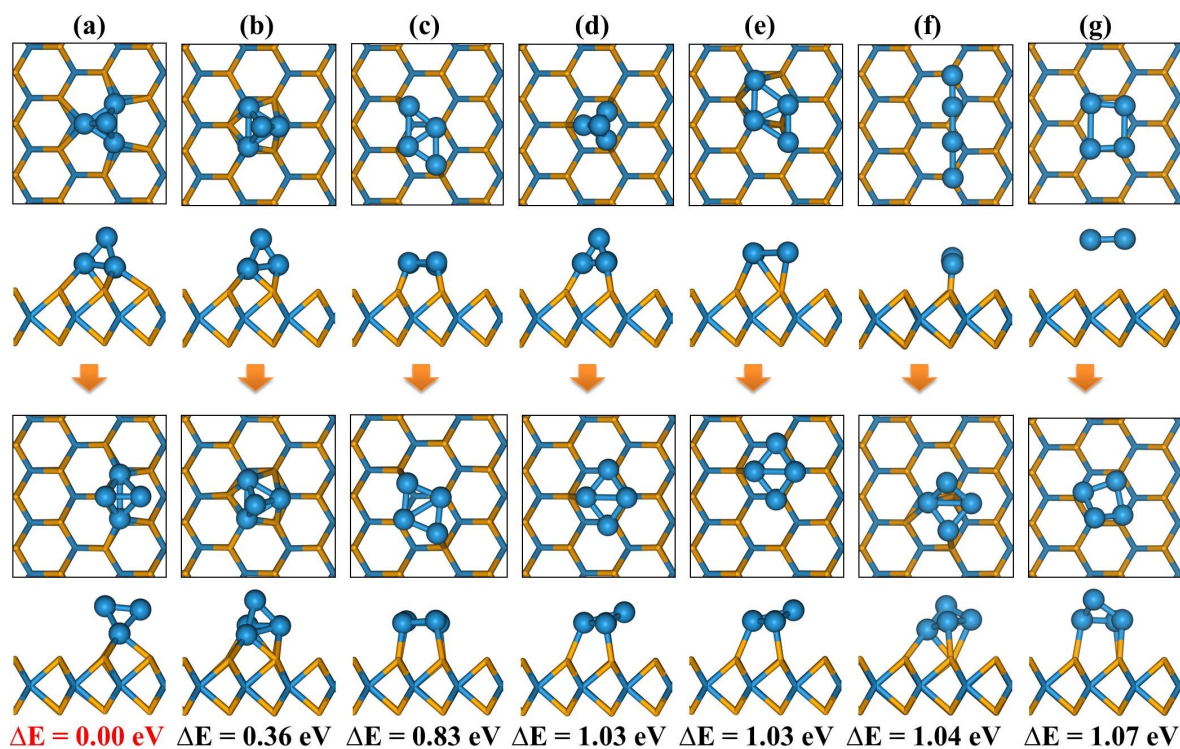


Figure S5. The top and side view of the initial adsorption of W_4 cluster on the seven possible adsorption sites (top panel) and the optimized adsorption configuration (bottom panel). The relative energy of the different configurations is also marked. The lowest energy is highlighted in red.

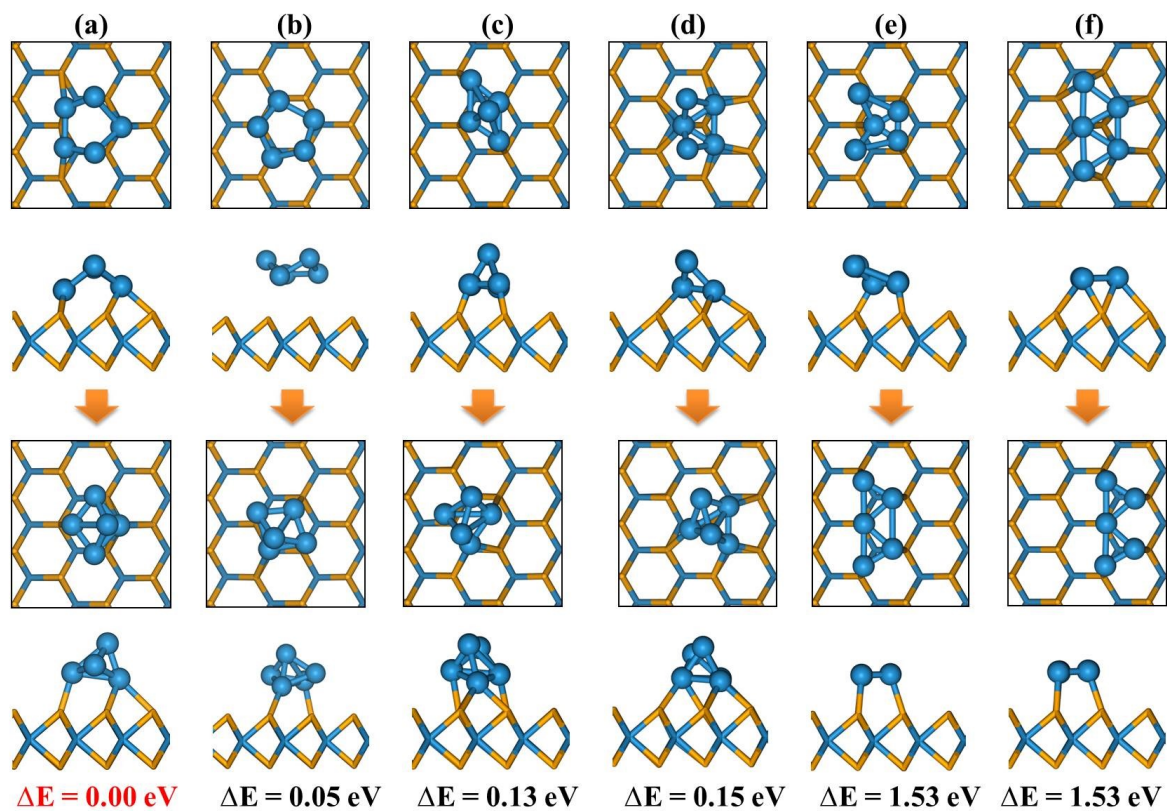


Figure S6. The top and side view of the initial adsorption of W_5 cluster on the six possible adsorption sites (top panel) and the optimized adsorption configuration (bottom panel). The relative energy of the different configurations is also marked. The lowest energy is highlighted in red.

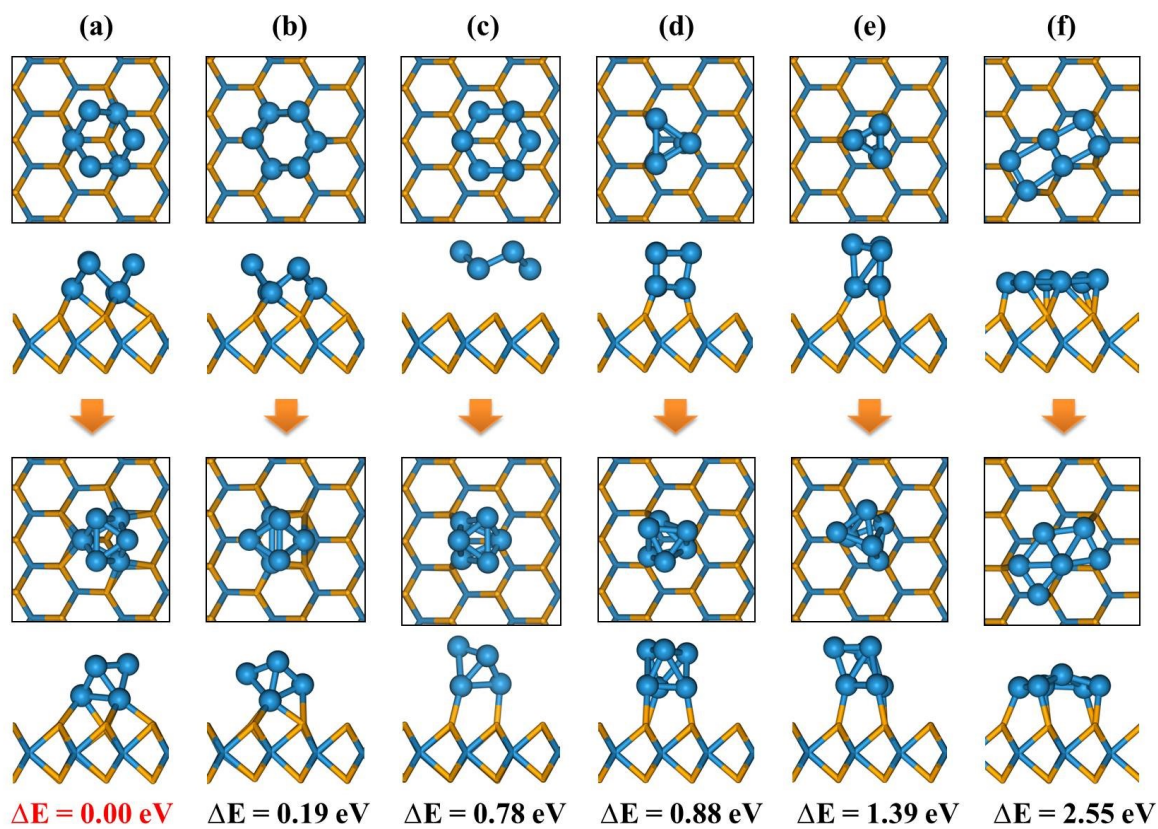


Figure S7. The top and side view of the initial adsorption of W_6 cluster on the six possible adsorption sites (top panel) and the optimized adsorption configuration (bottom panel). The relative energy of the different configurations is also marked. The lowest energy is highlighted in red.

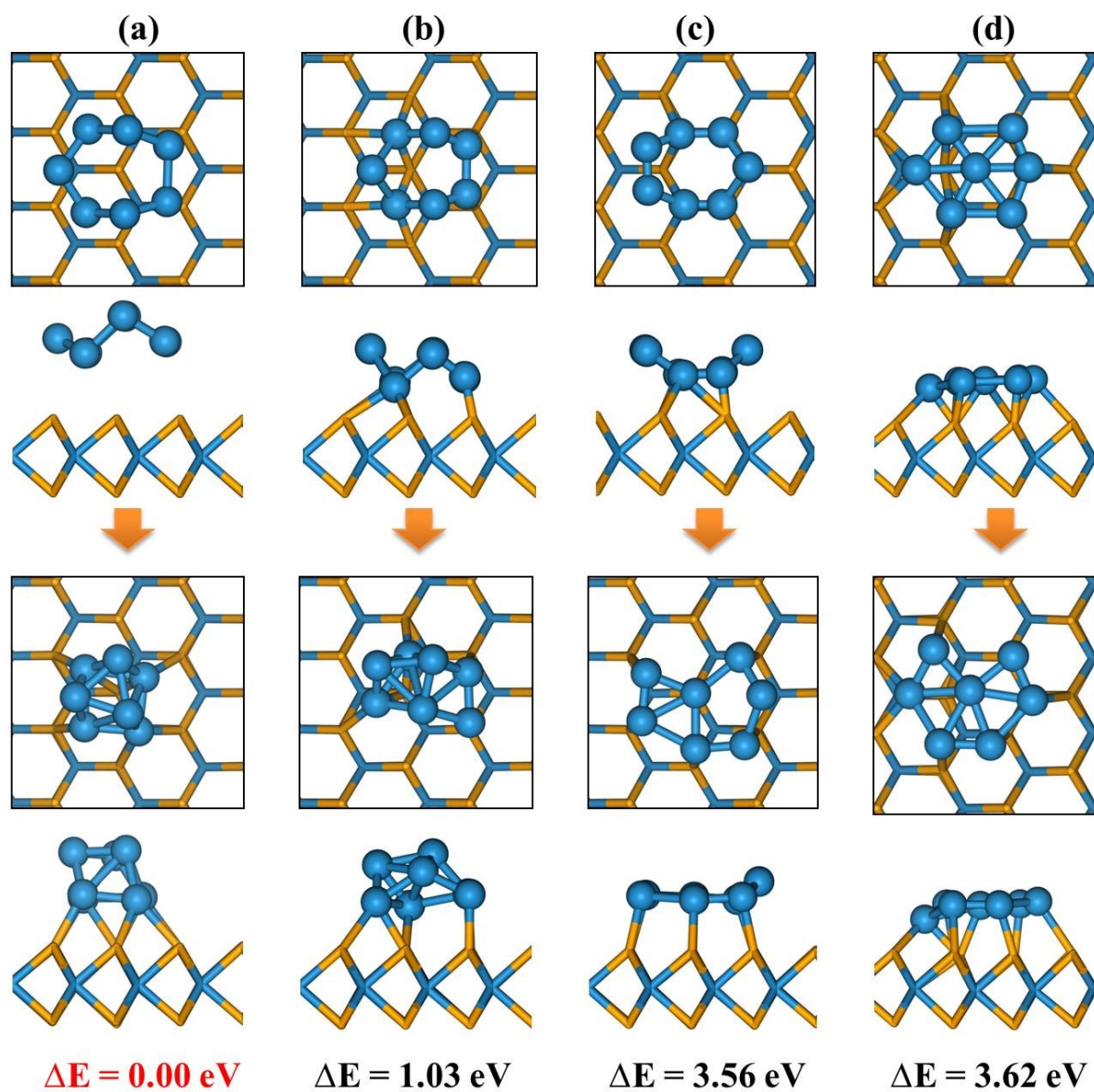


Figure S8. The top and side view of the initial adsorption of W_7 cluster on the four possible adsorption sites (top panel) and the optimized adsorption configuration (bottom panel). The relative energy of the different configurations is also marked. The lowest energy is highlighted in red.

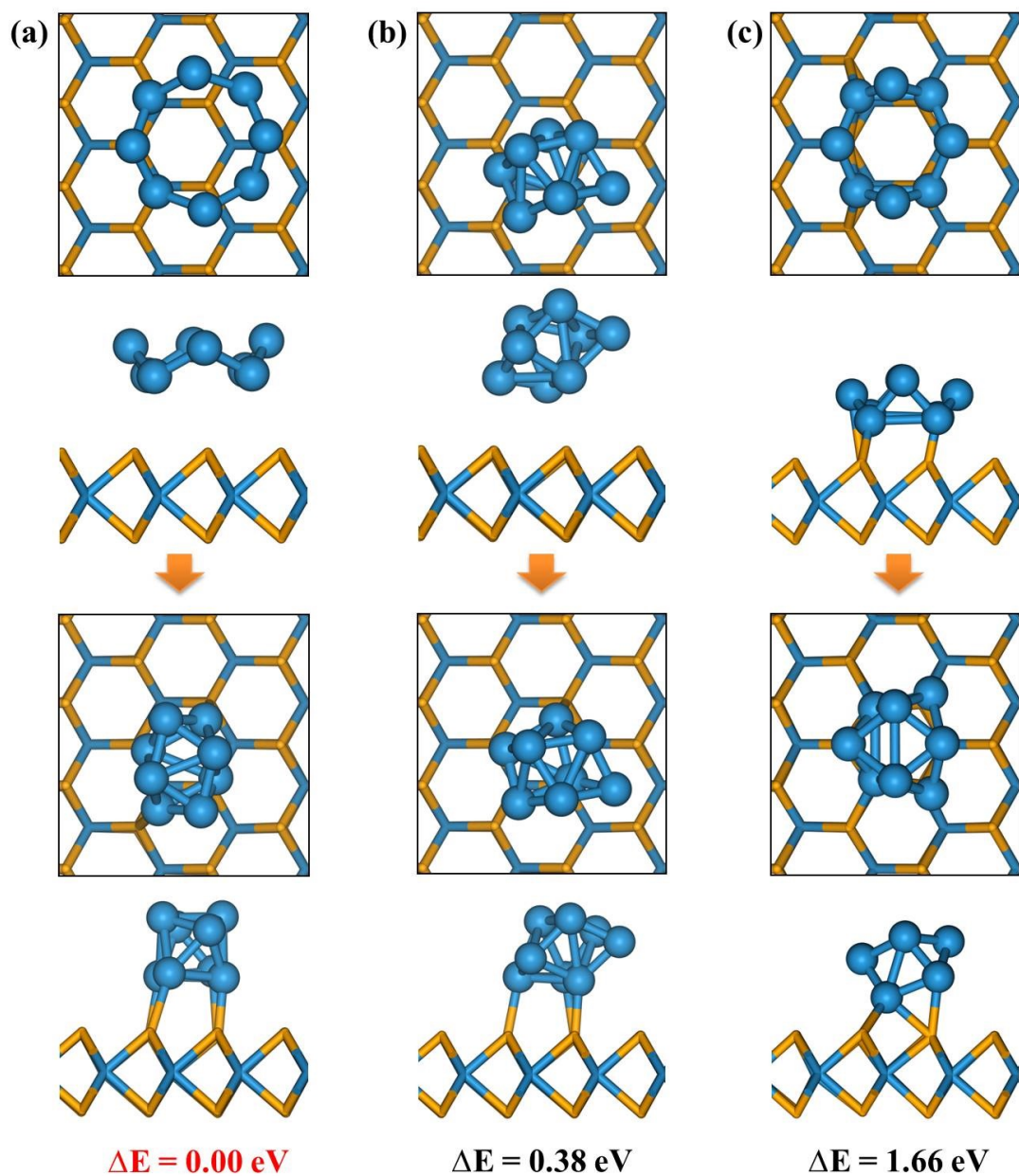


Figure S9. The top and side view of the initial adsorption of W_8 cluster on the three possible adsorption sites (top panel) and the optimized adsorption configuration (bottom panel). The relative energy of the different configurations is also marked. The lowest energy is highlighted in red.

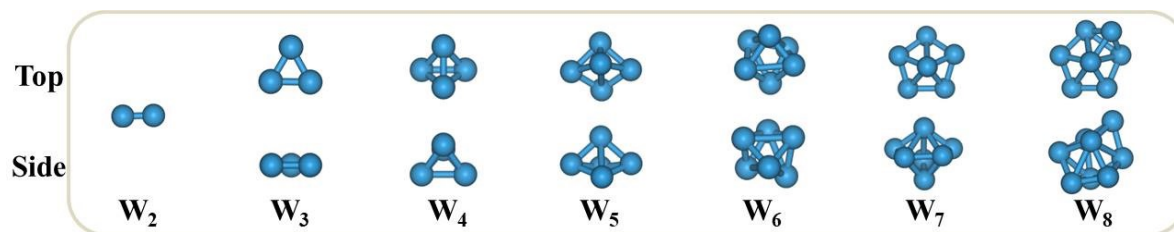


Figure S10. The top and side view of W_N ($N = 2-8$) cluster in vacuum.

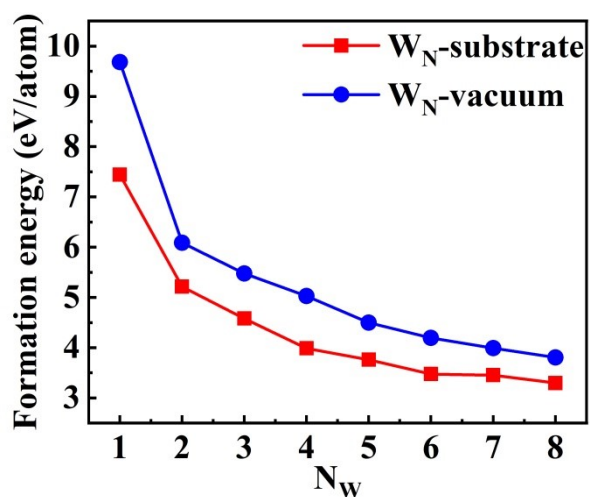


Figure S11. The formation energy of W_N ($N = 1-8$) clusters in vacuum and on substrate.

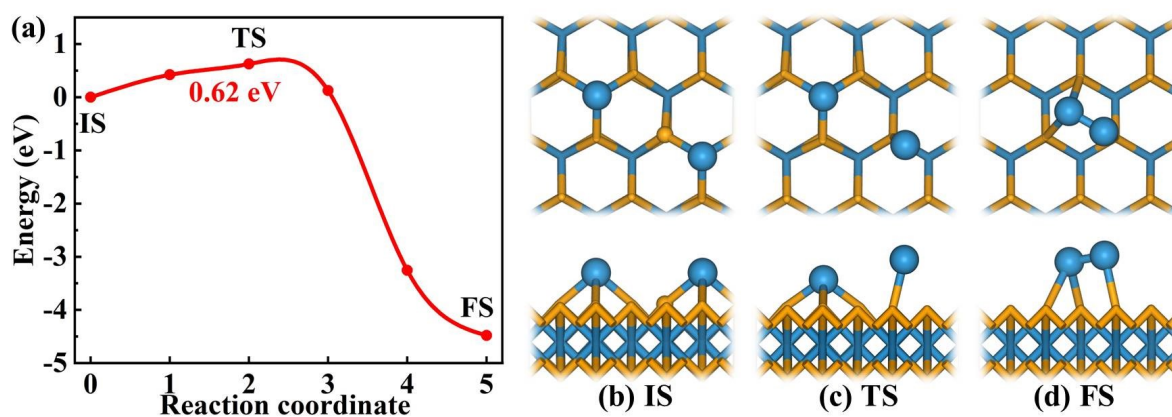


Figure S12. (a) The diffusion barrier of the W atom on the substrate. The top and side views of (a) initial state (IS), (c) transition state (TS) and (d) final state (FS).

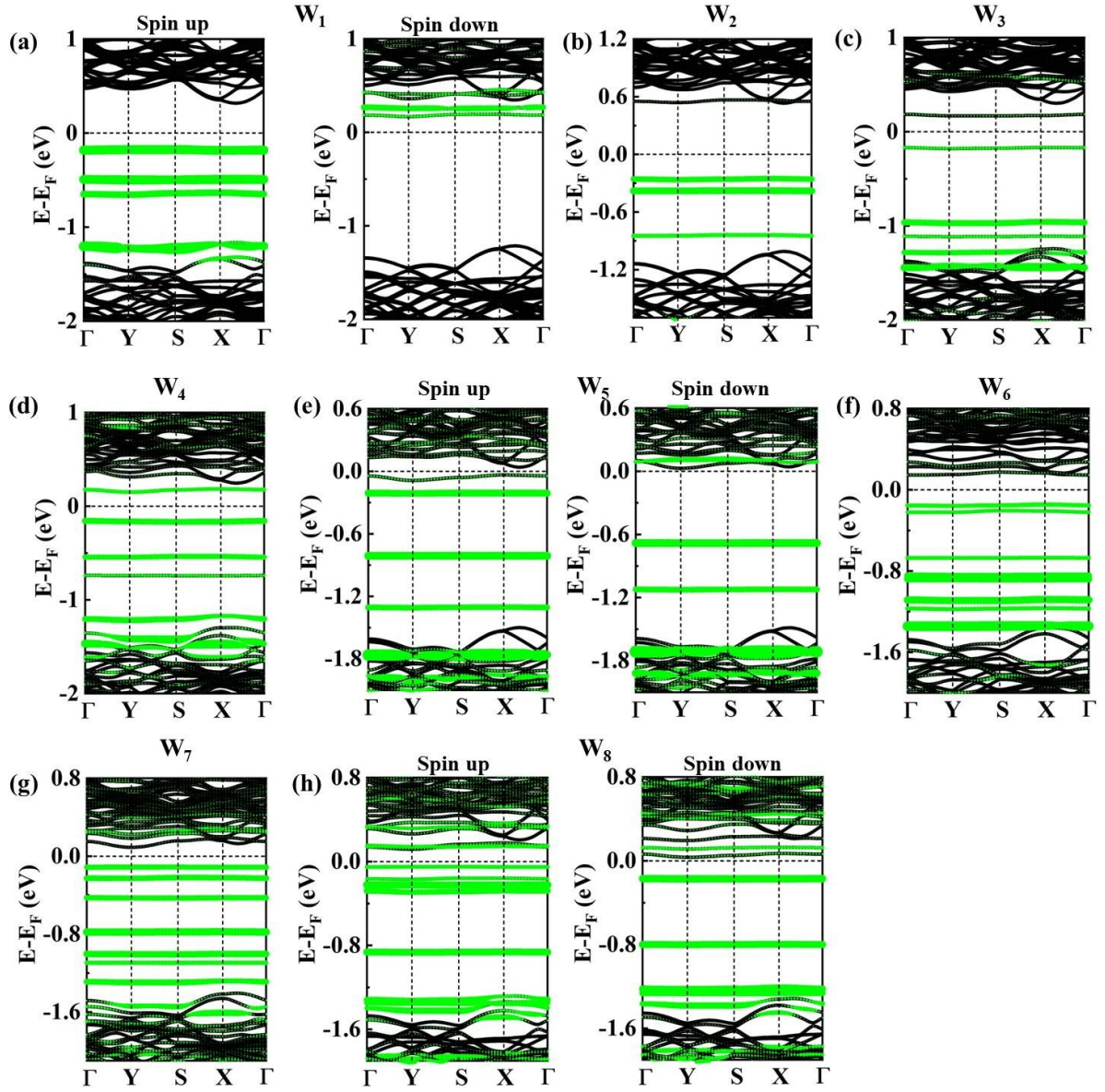


Figure S13. (a-h) The projected band structures of monolayer WSe_2 with W_N ($N= 1-8$) clusters on the surface. Electronic states projected on W_N clusters are marked by the green color circles.

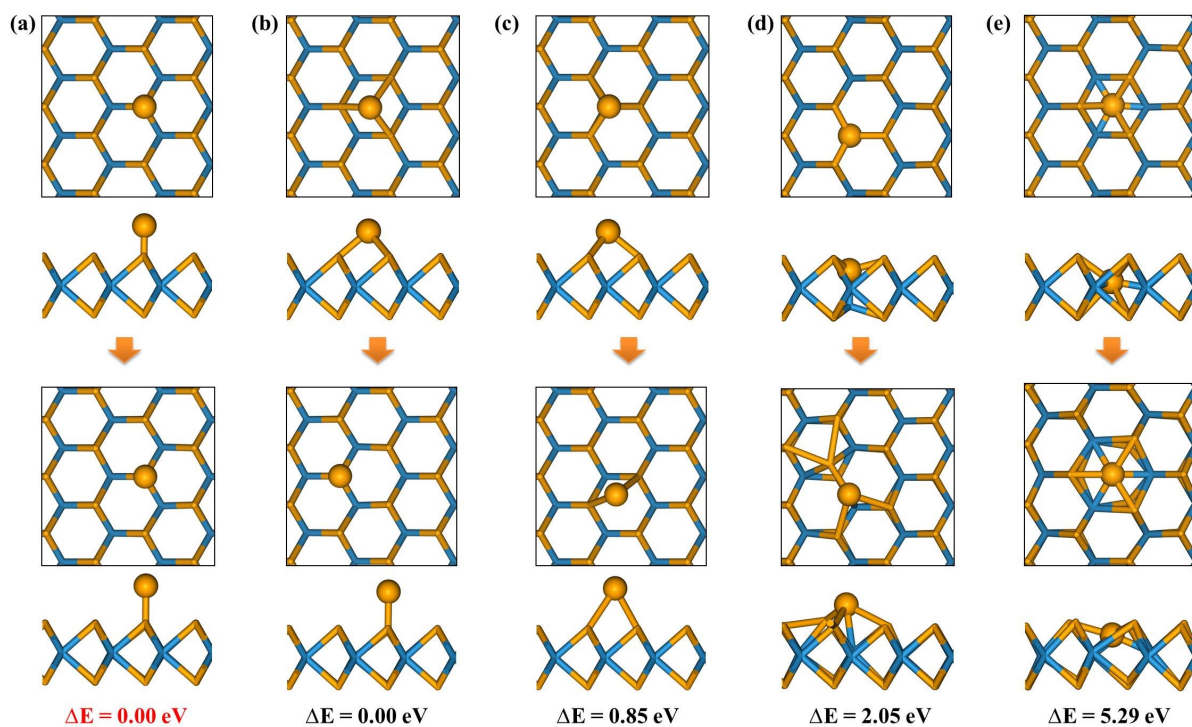


Figure S14. The top and side view of the initial adsorption of single Se atoms on the five different adsorption sites (top panel) and the optimized adsorption configuration (bottom panel). The relative energy of the different configurations is also marked. The lowest energy is highlighted in red.

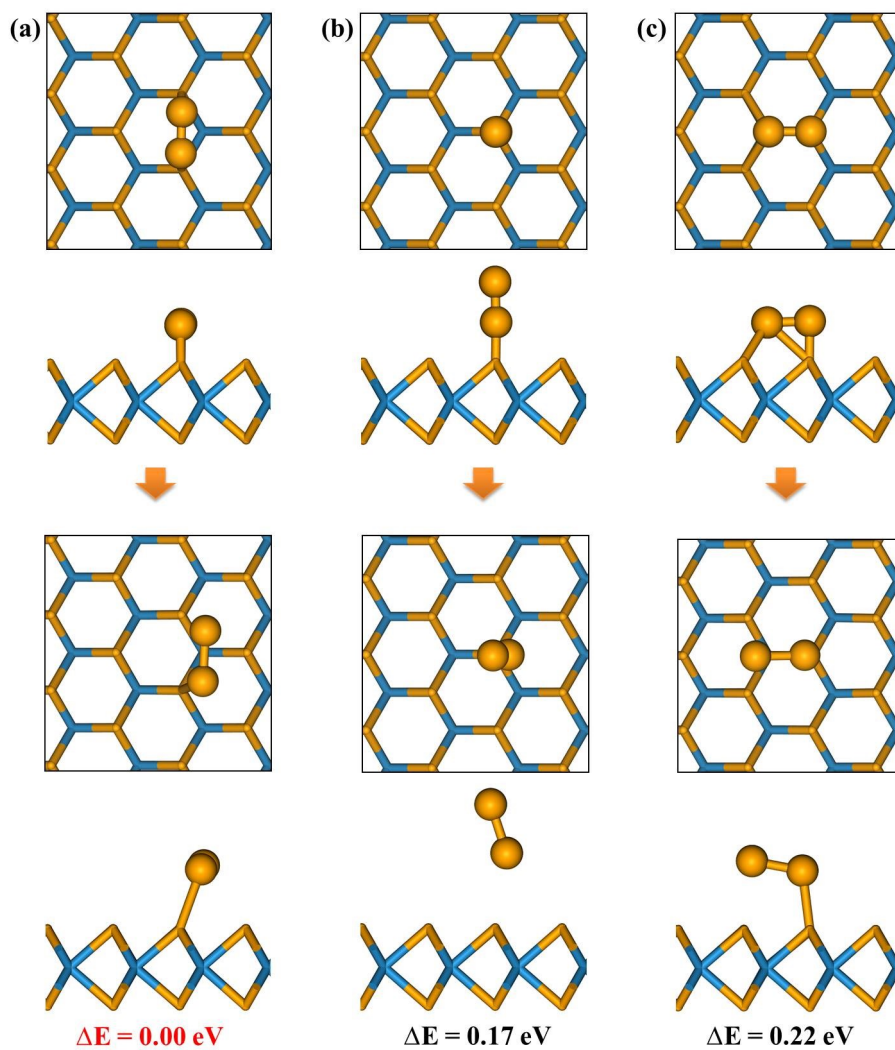


Figure S15. The top and side view of the initial adsorption of Se_2 cluster on the three different adsorption sites (top panel) and the optimized adsorption configuration (bottom panel). The relative energy of the different configurations is also marked. The lowest energy is highlighted in red.

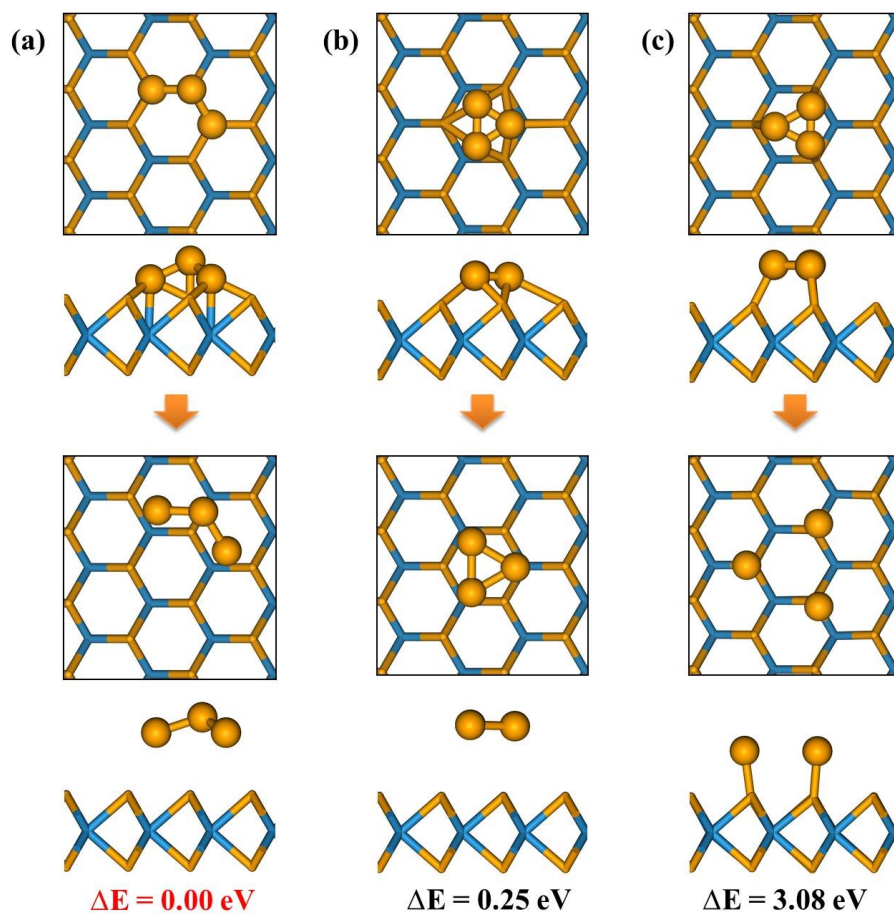


Figure S16. The top and side view of the initial adsorption of Se_3 cluster on the three different adsorption sites (top panel) and the optimized adsorption configuration (bottom panel). The relative energy of the different configurations is also marked. The lowest energy is highlighted in red.

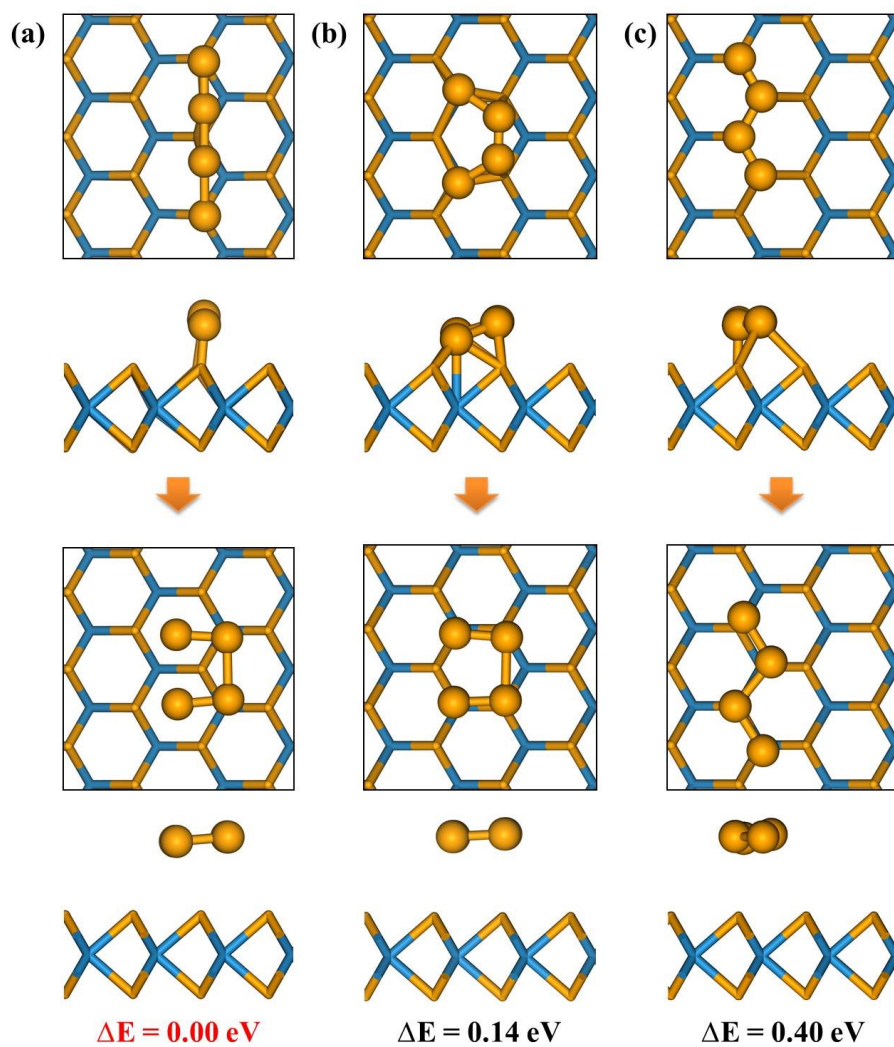


Figure S17. The top and side view of the initial adsorption of Se_4 cluster on the three different adsorption sites (top panel) and the optimized adsorption configuration (bottom panel). The relative energy of the different configurations is also marked. The lowest energy is highlighted in red.

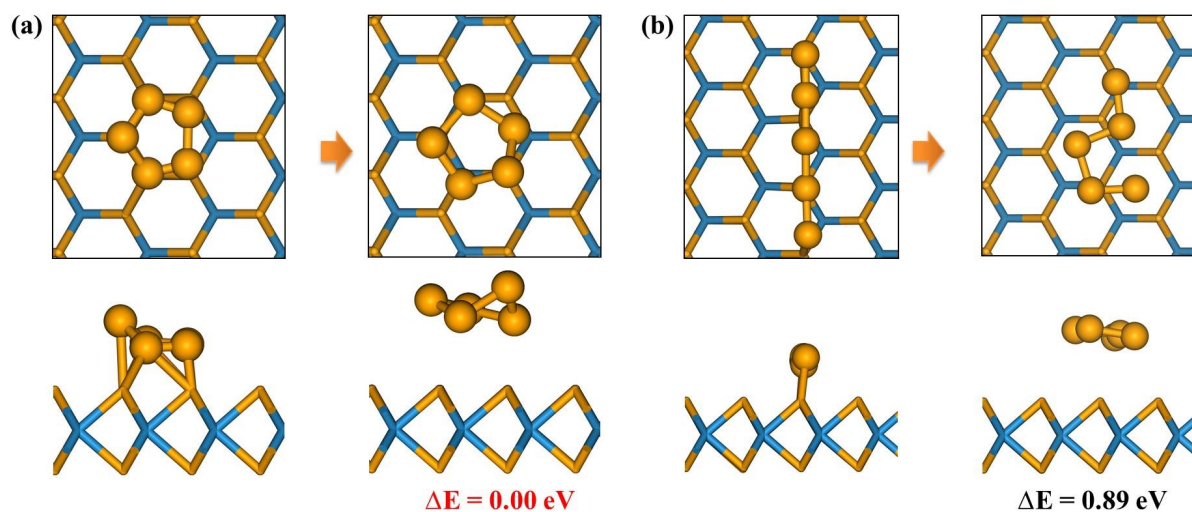


Figure S18. The top and side view of the initial adsorption of Se₅ cluster on the two different adsorption sites (left panel) and the optimized adsorption configuration (right panel). The relative energy of the different configurations is also marked. The lowest energy is highlighted in red.

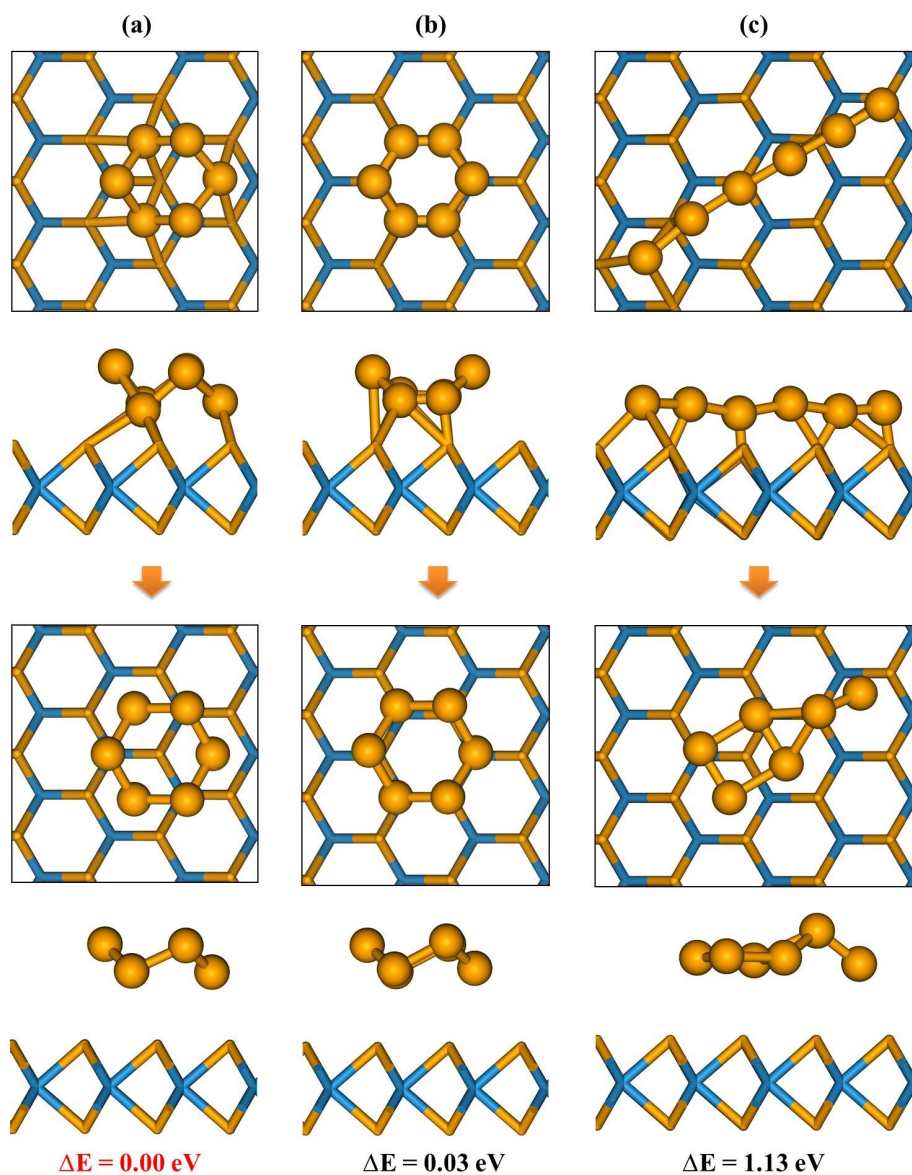


Figure S19. The top and side view of the initial adsorption of Se₆ cluster on the three different adsorption sites (top panel) and the optimized adsorption configuration (bottom panel). The relative energy of the different configurations is also marked. The lowest energy is highlighted in red.

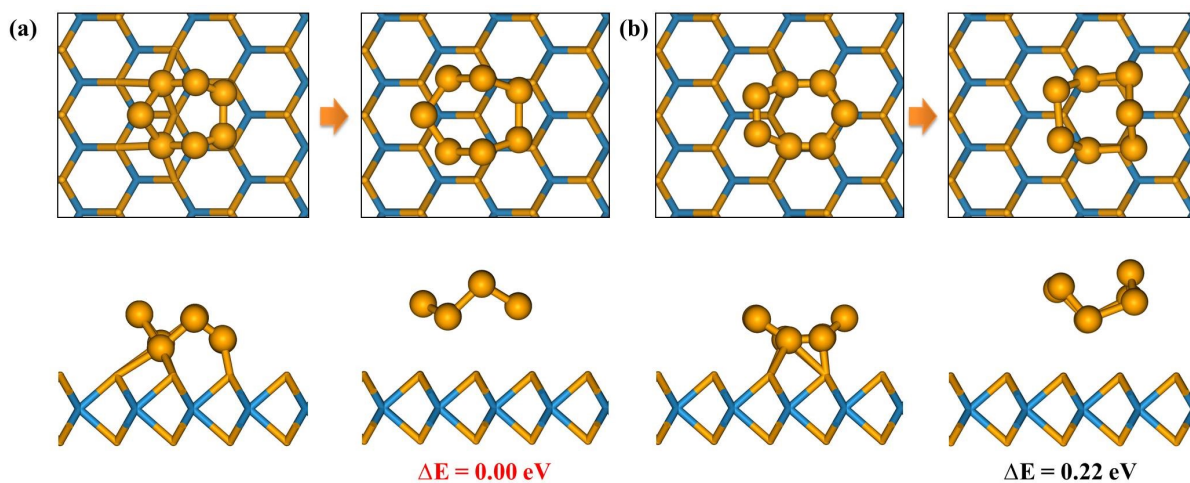


Figure S20. The top and side view of the initial adsorption of Se_7 cluster on the two different adsorption sites (left panel) and the optimized adsorption configuration (right panel). The relative energy of the different configurations is also marked. The lowest energy is highlighted in red.

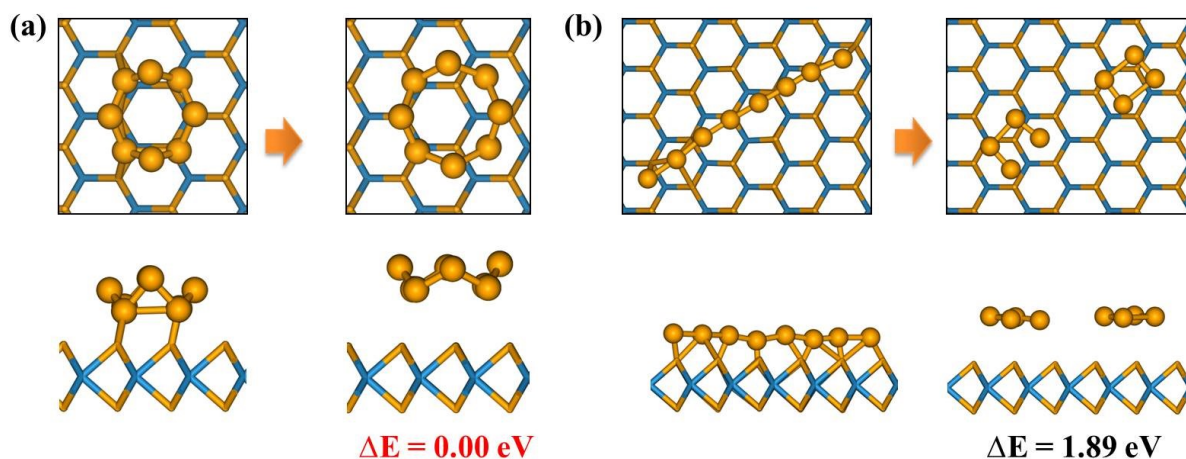


Figure S21. The top and side view of the initial adsorption of Se_8 cluster on the two different adsorption sites (left panel) and the optimized adsorption configuration (right panel). The relative energy of the different configurations is also marked. The lowest energy is highlighted in red.

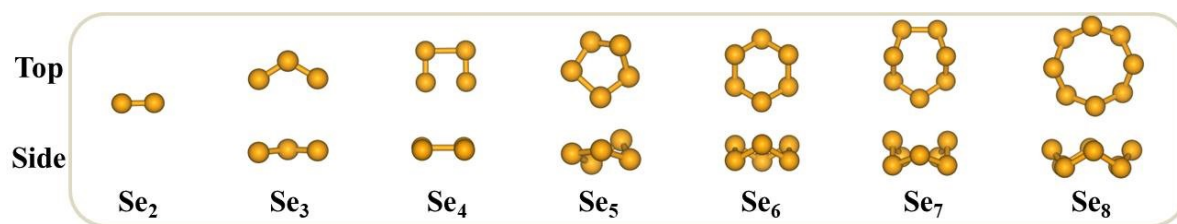


Figure S22. The top and side view of Se_N ($N = 2-8$) cluster in vacuum.

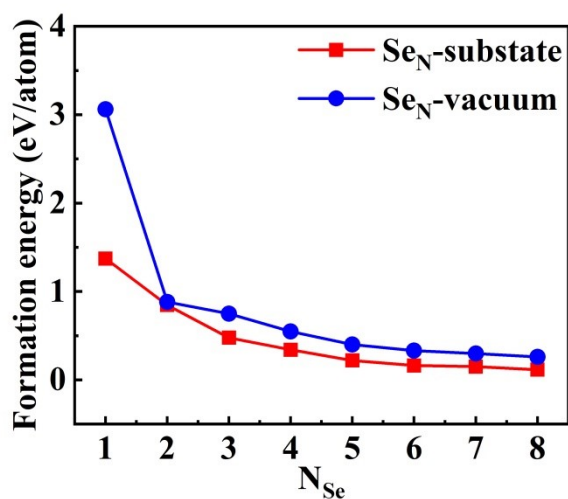


Figure S23. The formation energy of Se_N ($N = 1-8$) clusters in vacuum and on substrate.

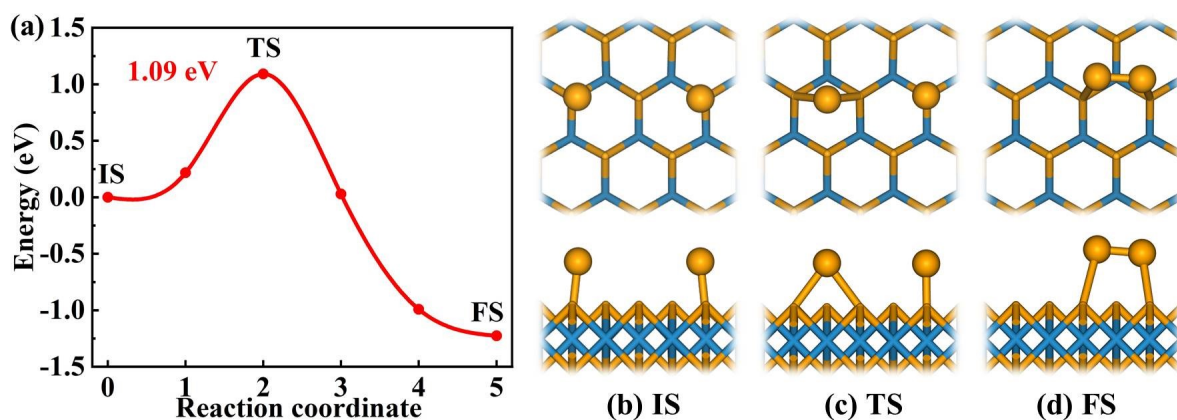


Figure S24. (a) The diffusion barrier of the Se atom on the substrate. The top and side views of (a) initial state (IS), (c) transition state (TS) and (d) final state (FS).

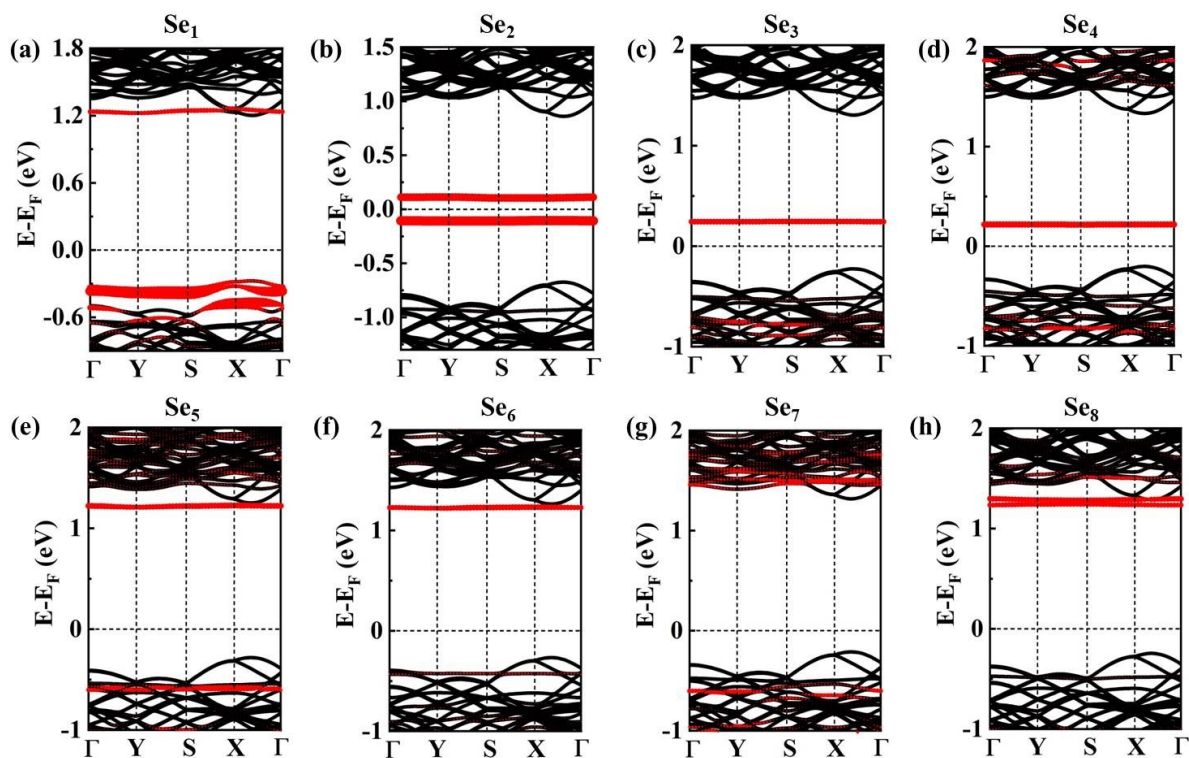


Figure S25. (a-h) The projected band structures of Se_N ($N = 1-8$) cluster adsorption on the substrate, respectively.

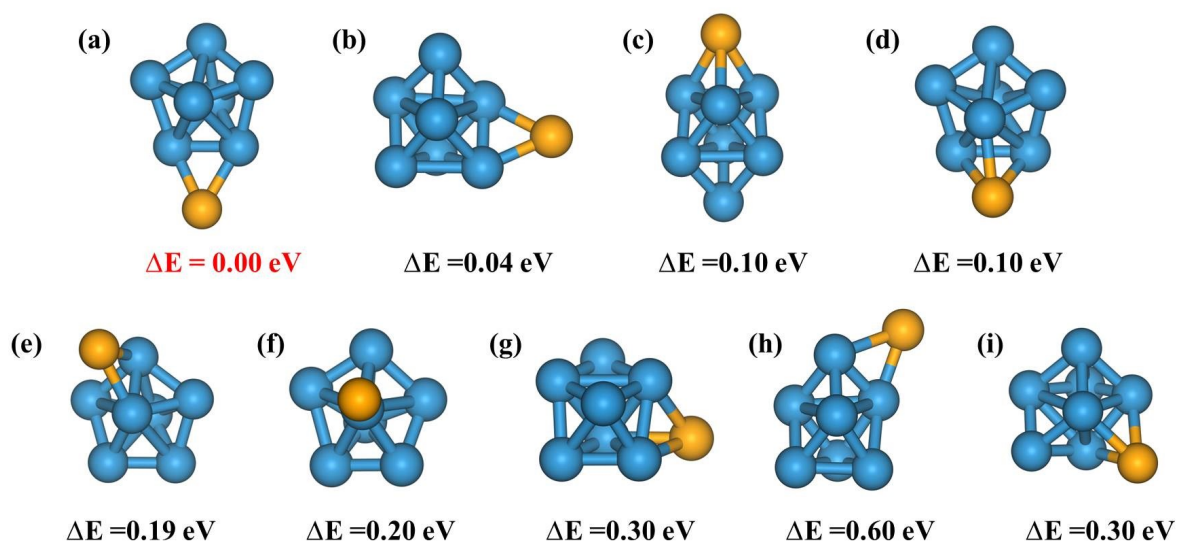


Figure S26. (a-i) The possible structure of the W_7Se_1 cluster in vacuum. The relative energy of the different configurations is also marked. The lowest energy is highlighted in red.

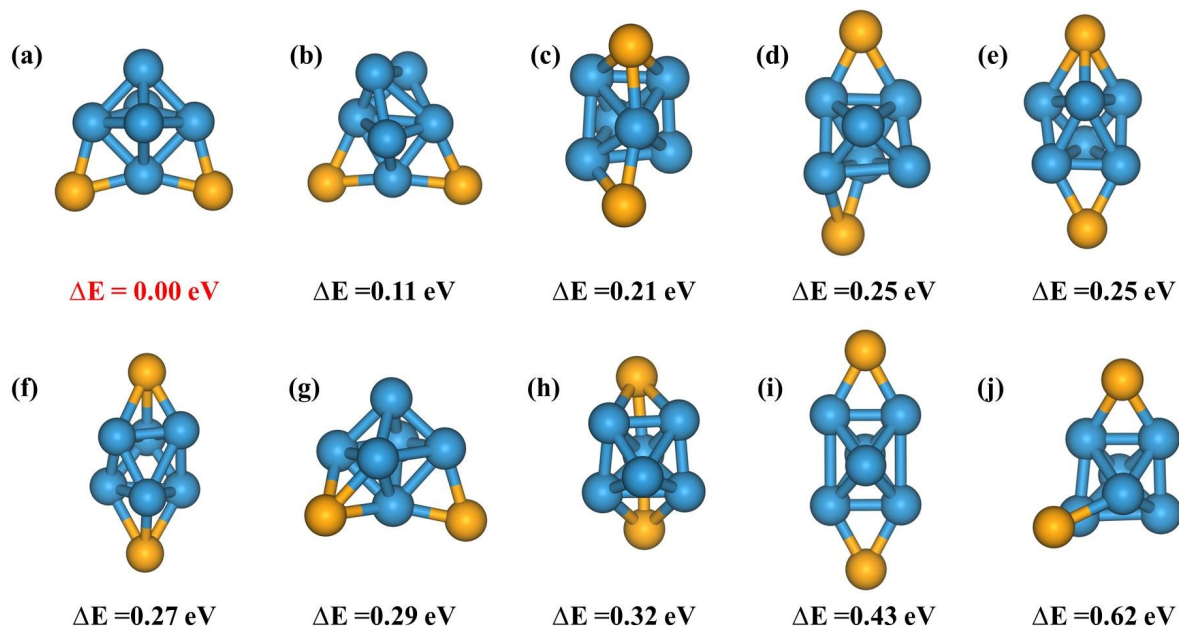


Figure S27. (a-j) The possible structure of the W_6Se_2 cluster in vacuum. The relative energy of the different configurations is also marked. The lowest energy is highlighted in red.

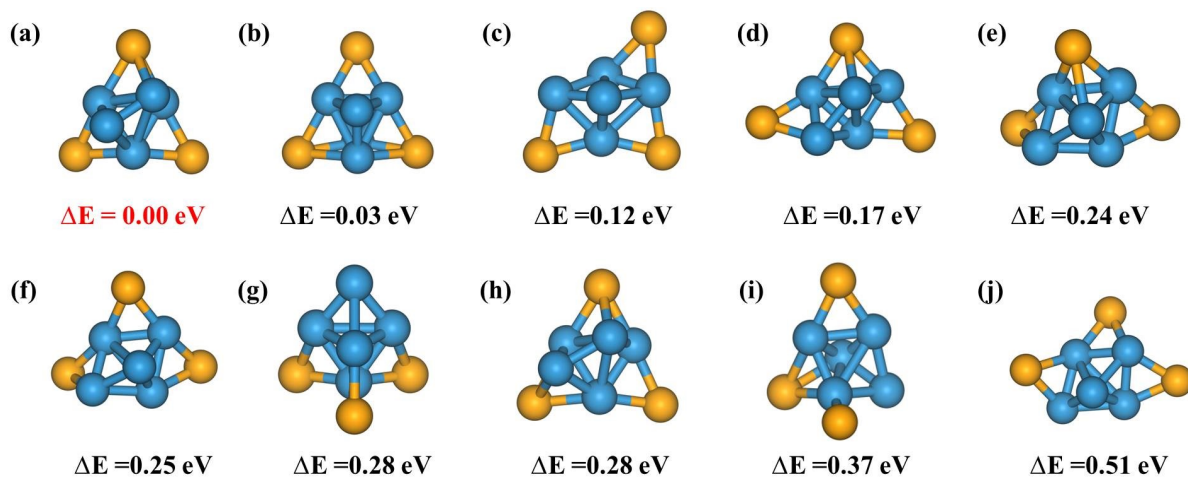


Figure S28. (a-j) The possible structure of the W_5Se_3 cluster in vacuum. The relative energy of the different configurations is also marked. The lowest energy is highlighted in red.

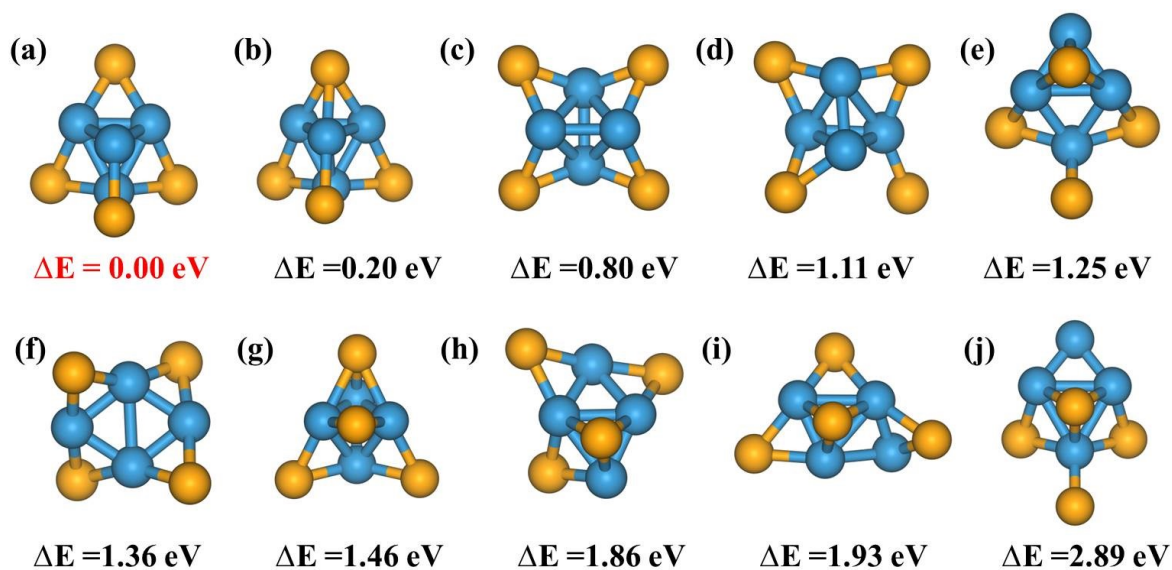


Figure S29. (a-j) The possible structure of the W_4Se_4 cluster in vacuum. The relative energy of the different configurations is also marked. The lowest energy is highlighted in red.

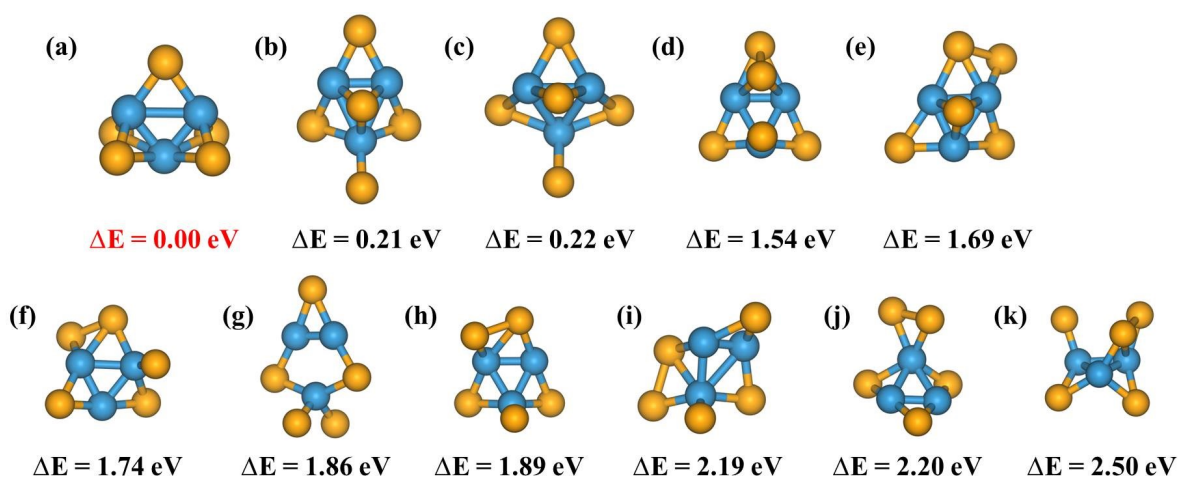


Figure S30. (a-k) The possible structure of the W_3Se_5 cluster in vacuum. The relative energy of the different configurations is also marked. The lowest energy is highlighted in red.

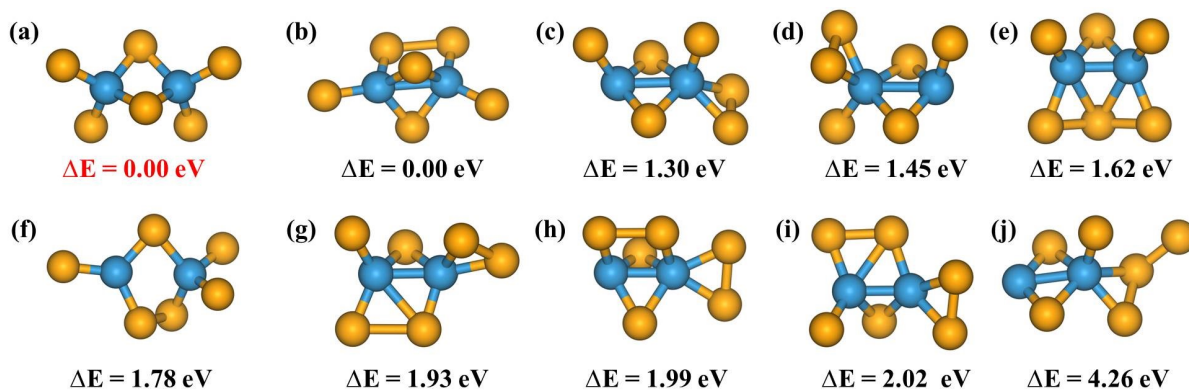


Figure S31. (a-k) The possible structure of the W_2Se_6 cluster in vacuum. The relative energy of the different configurations is also marked. The lowest energy is highlighted in red.

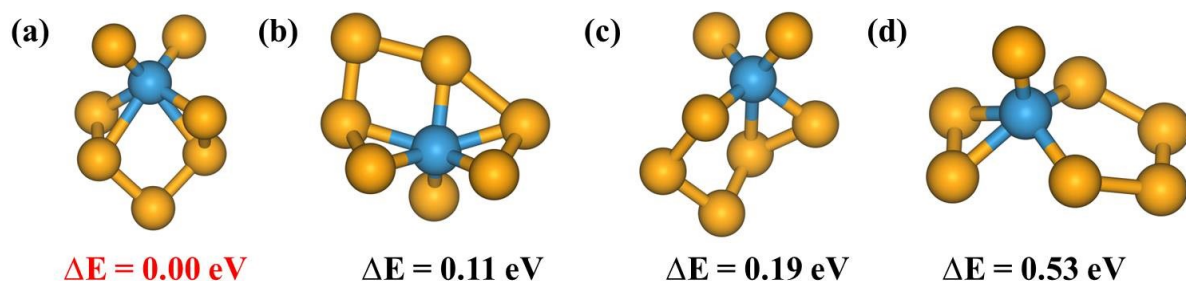


Figure S32. (a-d) The possible structure of the W_1Se_7 cluster in vacuum. The relative energy of the different configurations is also marked. The lowest energy is highlighted in red.

In vacuum, W_7Se_1 cluster is composed of the bare GS structure of the W_7 cluster and a Se atom bond with two W atoms. The GS W_7Se_2 cluster is composed by the GS W_6 cluster and two Se atoms adsorption on the bridge site of two W-W bonds. The GS structure of W_5Se_3 is composed by GS W_5 cluster and two Se atoms on the top of W-W bond and each Se atom bond with two W atoms and one Se atom on the top of W-W-W plane and bond with three W atoms. The GS structure of W_4Se_4 cluster is composed by the GS W_4 cluster and other four Se atoms adsorption on the top of W-W bond and each Se atom bond with two W atoms. The GS W_3Se_5 cluster is composed by GS W_3 cluster and five Se atoms prefer bond with the bridge of W-W bond. In the GS structure of W_2Se_6 cluster, each W atom is bond with four Se atoms. In the GS structure of W_2Se_6 clusters in vacuum, the W atom bonded with six Se atoms.

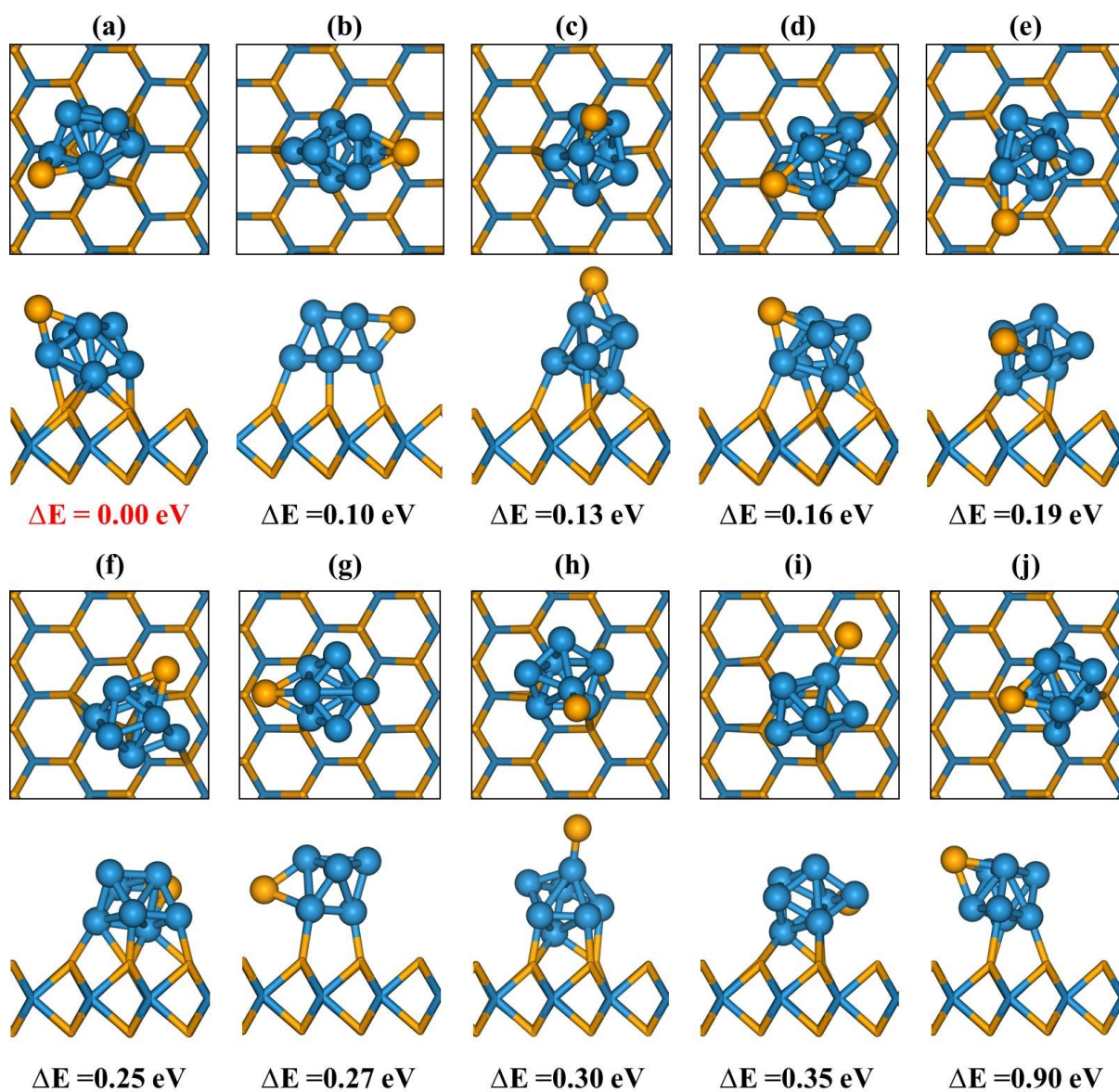


Figure S33. (a-j) The possible structure of the W_7Se_1 cluster on substrate. The relative energy of the different configurations is also marked. The lowest energy is highlighted in red.

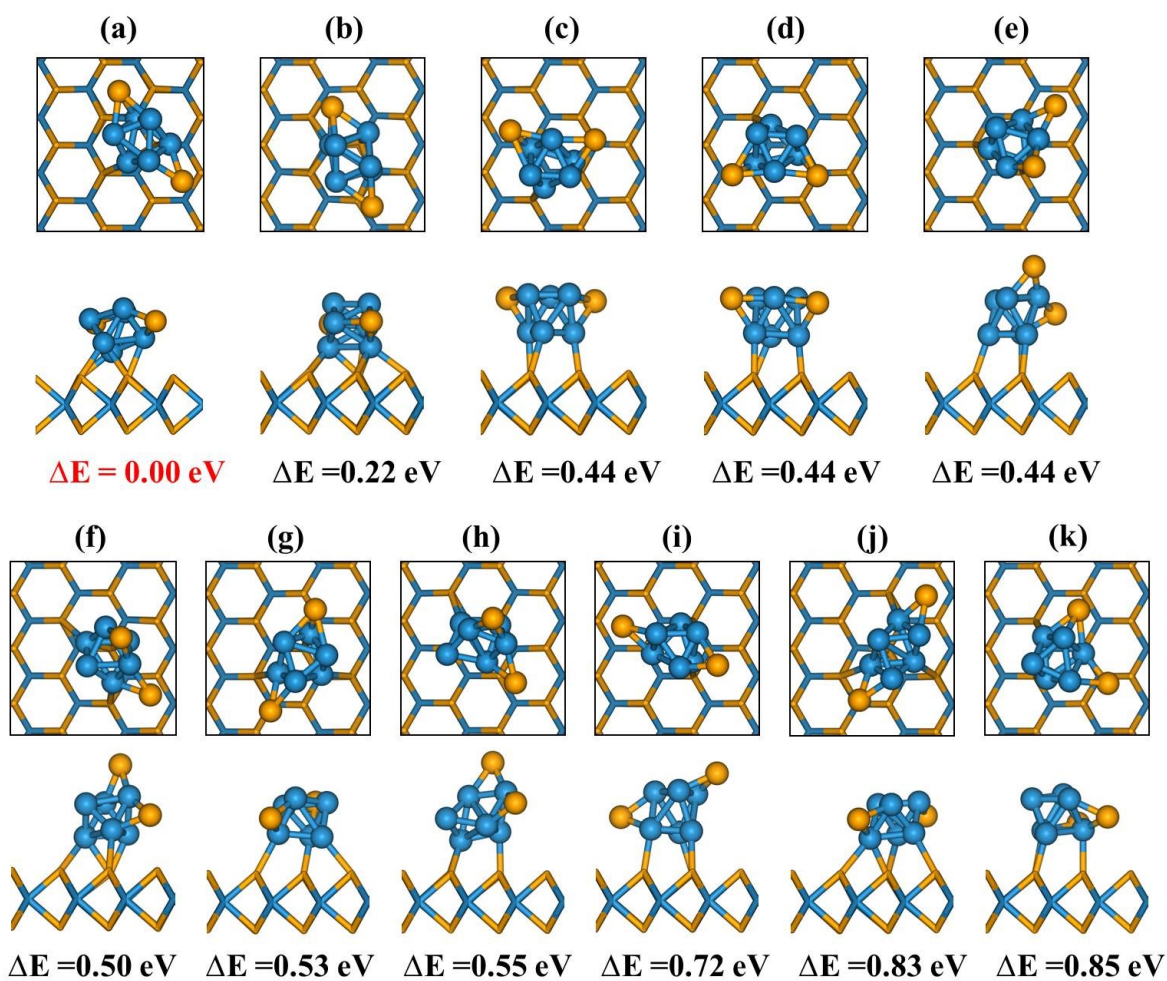


Figure S34. (a-k) The possible structure of the W_6Se_2 cluster on substrate. The relative energy of the different configurations is also marked. The lowest energy is highlighted in red.

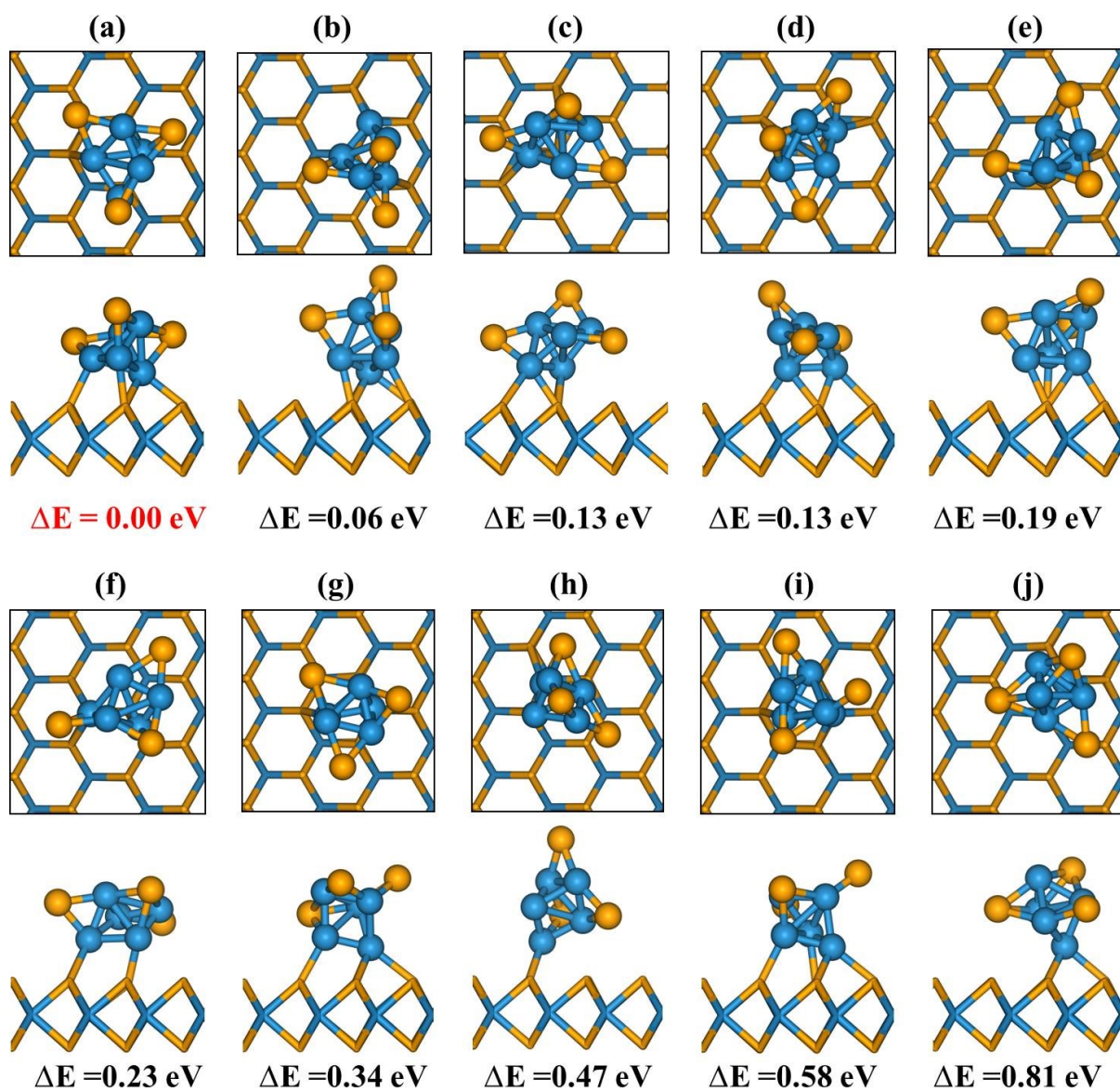


Figure S35. (a-j) The possible structure of the W_5Se_3 cluster on substrate. The relative energy of the different configurations is also marked. The lowest energy is highlighted in red.

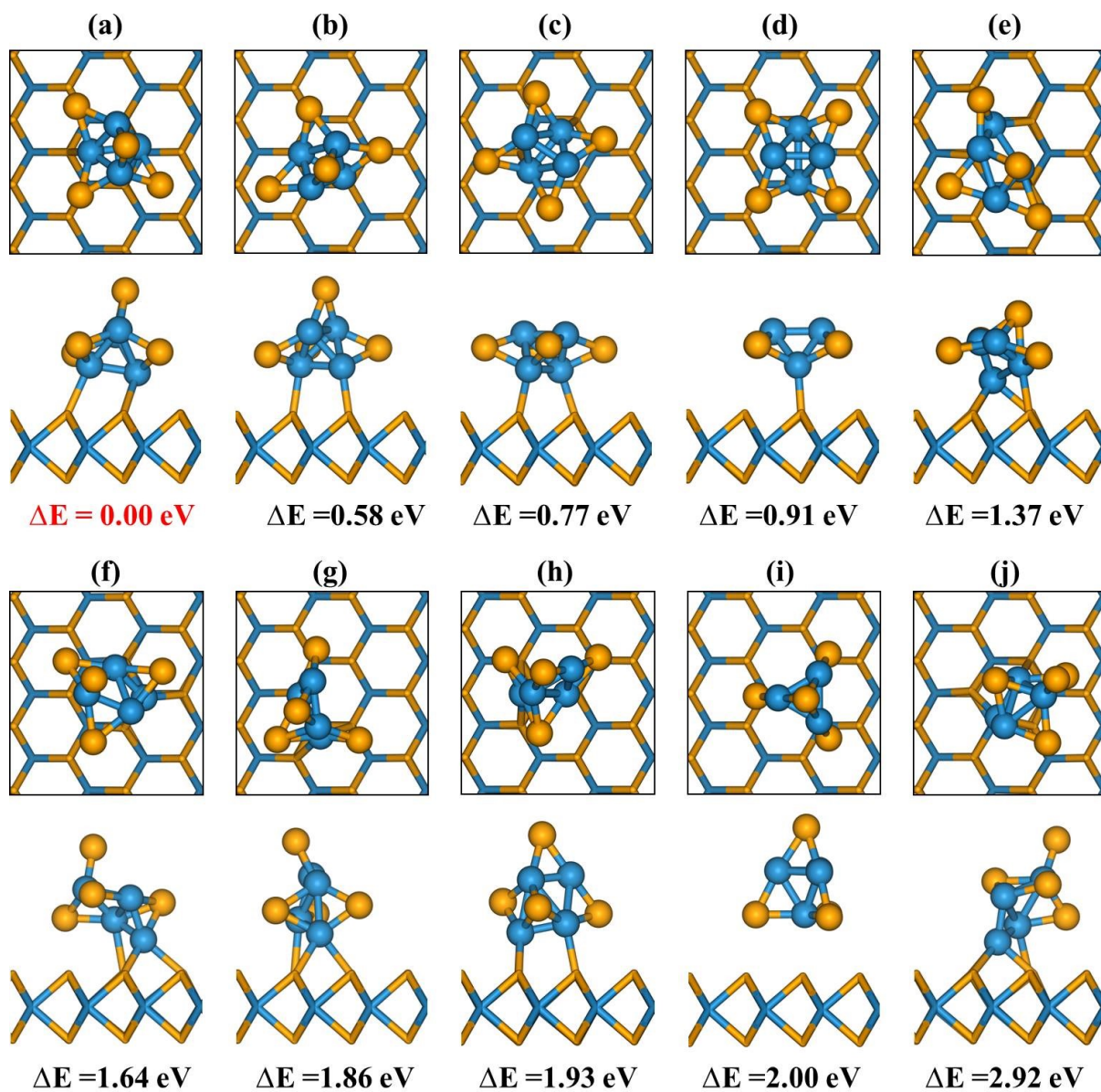


Figure S36. (a-j) The possible structure of the W_4Se_4 cluster on substrate. The relative energy of the different configurations is also marked. The lowest energy is highlighted in red.

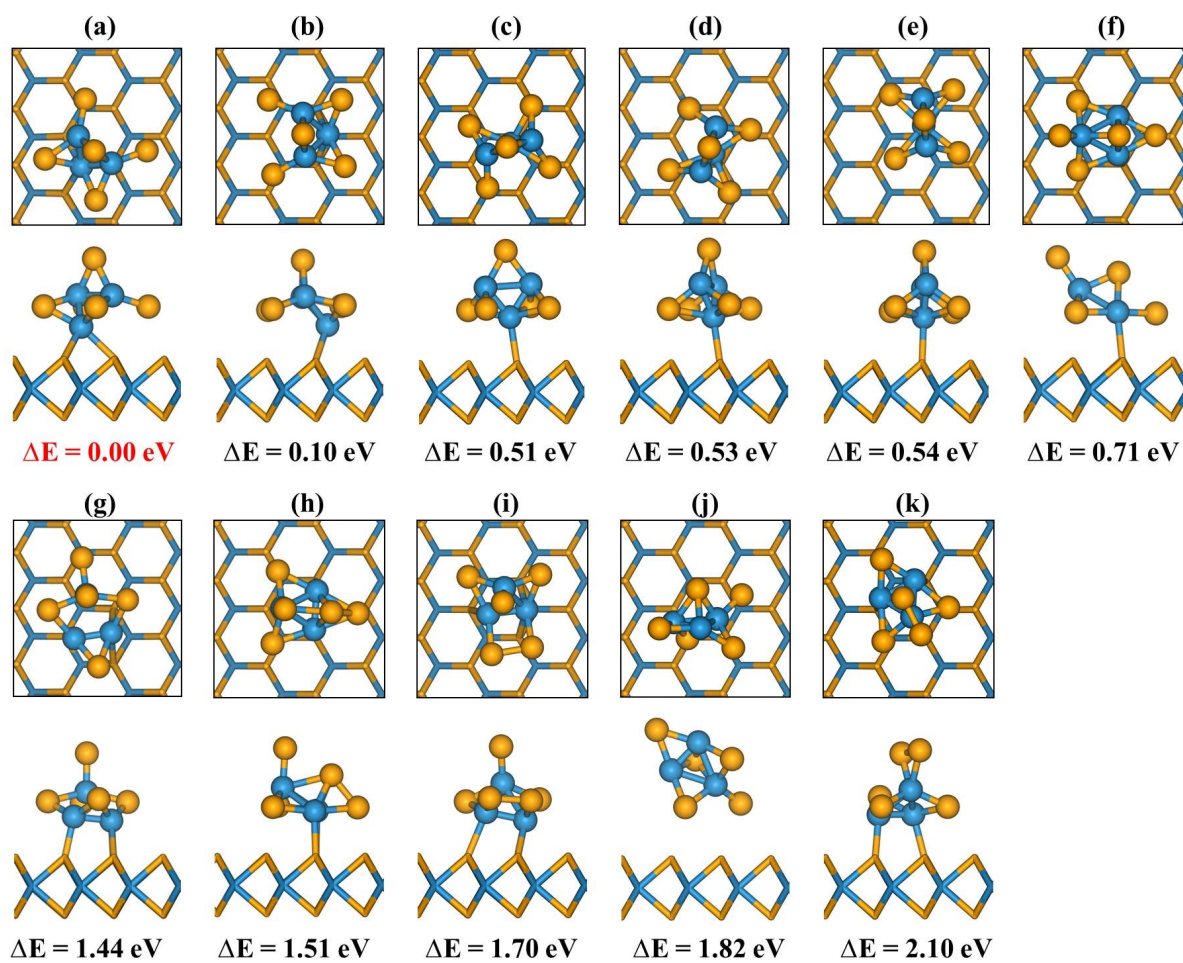


Figure S37. (a-k) The possible structure of the W_3Se_5 cluster on substrate. The relative energy of the different configurations is also marked. The lowest energy is highlighted in red.

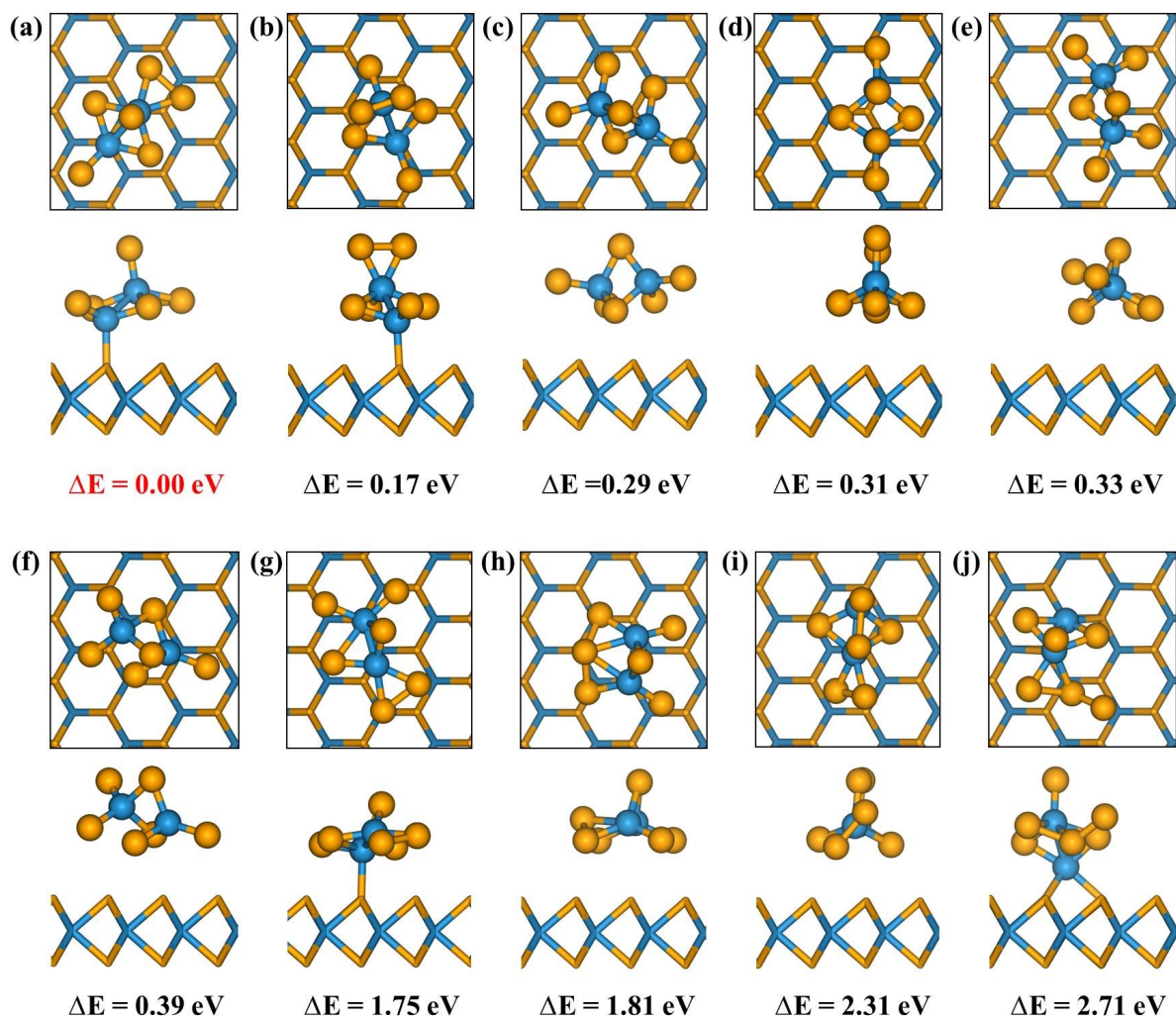


Figure S38. (a-j) The possible structure of the W_2Se_6 cluster on substrate. The relative energy of the different configurations is also marked. The lowest energy is highlighted in red.

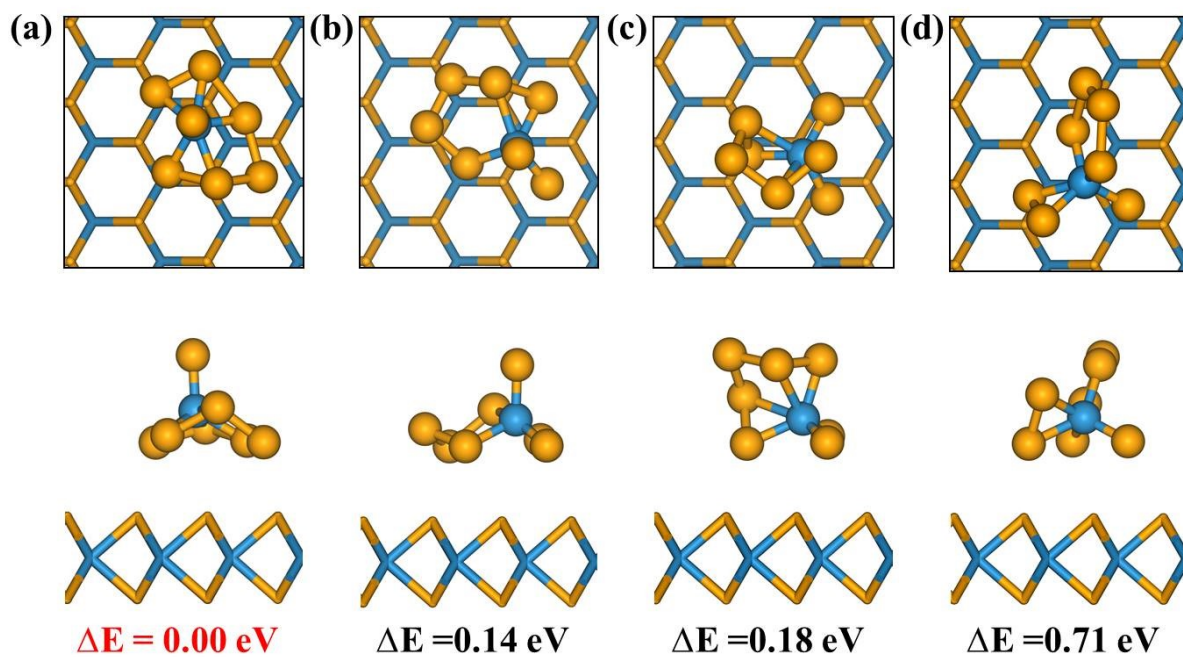


Figure S39. (a-d) The possible structure of the W_1Se_7 cluster on substrate. The relative energy of the different configurations is also marked. The lowest energy is highlighted in red.

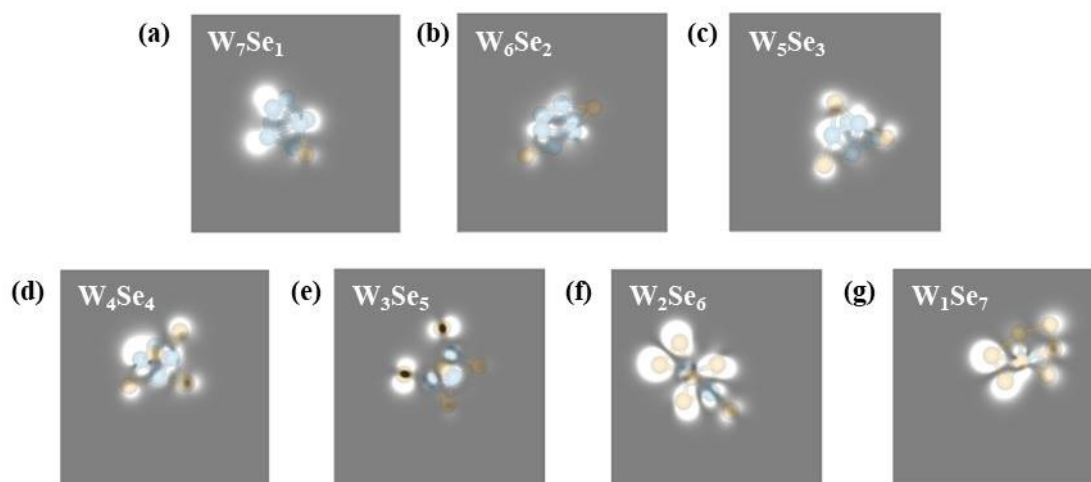


Figure S40. The simulated STM of $W_{8-N}Se_N$ ($N = 1-7$) clusters adsorption on the WSe_2 surface at -0.6 V bias, respectively.

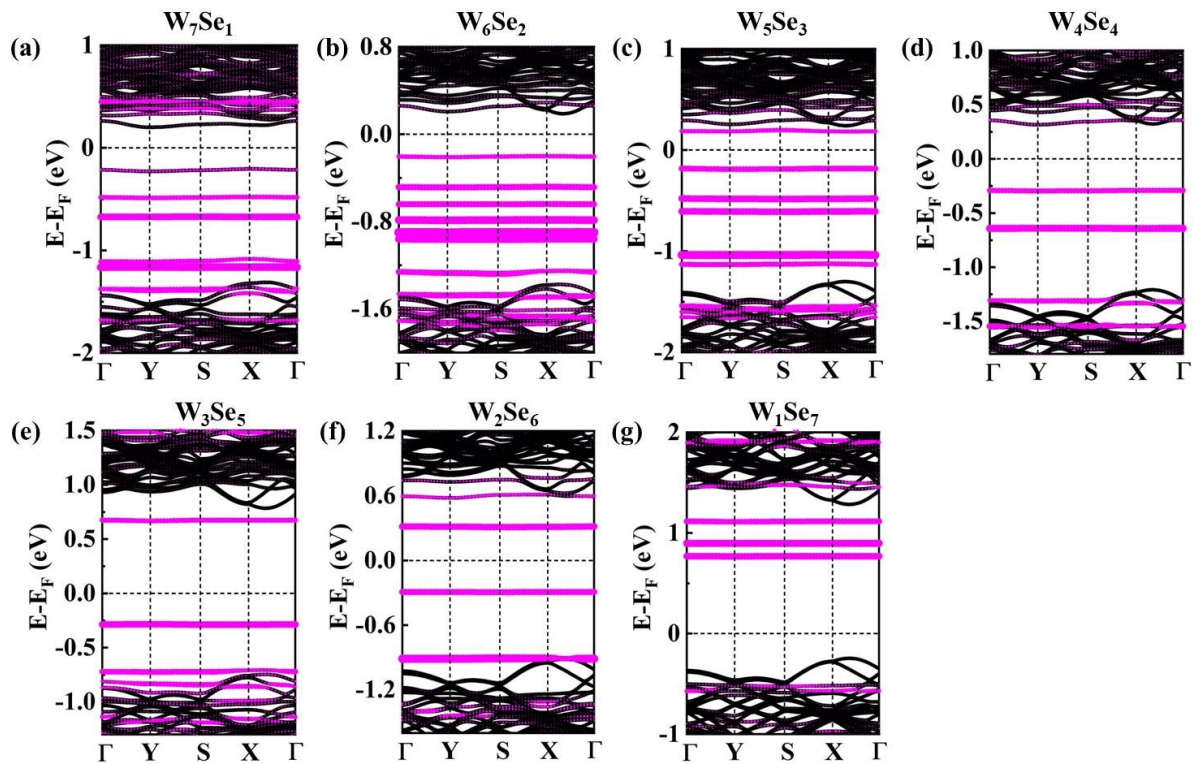


Figure S41. (a-h) The projected band structures of $W_{8-N}Se_N$ ($N = 1-7$) cluster adsorption on the substrate. The electronic states projected on $W_{8-N}Se_N$ ($N = 1-8$) clusters are marked by pink color.

Table S1. The distance (d) between the scan tip and the Se_N , W_N ($N= 1-8$) and $\text{W}_{8-N}\text{Se}_N$ ($N = 1-7$) cluster in STM simulation.

Cluster	d (Å)	Cluster	d (Å)	Cluster	d (Å)
W_1	0.19	Se_1	0.62	W_7Se_1	0.10
W_2	0.22	Se_2	0.15	W_6Se_2	0.46
W_3	0.20	Se_3	1.56	W_5Se_3	0.13
W_4	0.20	Se_4	0.20	W_4Se_4	0.17
W_5	0.20	Se_5	0.89	W_3Se_5	0.12
W_6	0.20	Se_6	0.28	W_2Se_6	0.08
W_7	0.20	Se_7	0.31	W_1Se_7	0.37
W_8	0.20	Se_8	0.27	-	-